NASA Contractor Report 185677

Hypersonic Three-Dimensional Nonequilibrium Boundary-Layer Equations in Generalized Curvilinear Coordinates

Jong-Hun Lee
BSA Services
Houston, Texas

Prepared for the
Lyndon B. Johnson Space Center
under contract NAS9-18493

February 1993

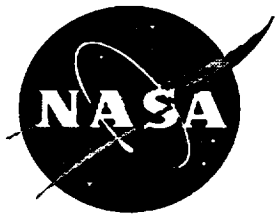

NASA Contractor Report 185677

Hypersonic Three-Dimensional Nonequilibrium Boundary-Layer Equations in Generalized Curvilinear Coordinates

Jong-Hun Lee

Contract NAS9-18493

February 1993

Table of Contents

Abstract

The basic governing equations for the second-order three-dimensional hypersonic thermal and chemical nonequilibrium boundary layer are derived by means of an order-of-magnitude analysis. A two-temperature concept is implemented into the system of boundary-layer equations by simplifying the rather complicated general three-temperature thermal gas model. The equations are written in a surface-oriented non-orthogonal curvilinear coordinate system, where two curvilinear coordinates are non-orthogonal and a third coordinate is normal to the surface. The equations are described with minimum use of tensor expressions arising from the coordinate transformation, to avoid unnecessary confusion for readers. The set of equations obtained will be suitable for the development of a three-dimensional nonequilibrium boundary-layer code. Such a code could be used to determine economically the aerodynamic/aerothermodynamic loads to the surfaces of hypersonic vehicles with general configurations. In addition, the basic equations for three-dimensional stagnation flow, of which solution is required as an initial value for space-marching integration of the boundary-layer equations, are given along with the boundary conditions, the boundary-layer parameters and the inner-outer layer matching procedure. Expressions for the chemical reaction rates and the thermodynamic and transport properties in the thermal nonequilibrium environment are explicitly given.

Nomenclature

$\underline{A}$	=	vector quantity
a	=	determinant of surface metric tensor
$\underline{a}_\alpha$, $\underline{a}^\alpha$	=	covariant and contravariant surface base vectors
$a_{\alpha\beta}$, $a^{\alpha\beta}$	=	surface metric tensor components
$b_{\alpha\beta}$	=	component of covariant surface curvature tensor
C_s	=	mass fraction of species s
c_p	=	frozen specific heat of mixture at constant pressure
$c_{pt,s}$	=	specific heat of species s at constant pressure for translational mode
c_{pel}	=	specific heat of mixture at constant pressure for electronic excitation
$c_{pel,s}$	=	specific heat of species s at constant pressure for electronic excitation
$c_{pr,s}$	=	specific heat of species s at constant pressure for rotational excitation
c_{pv}	=	specific heat of mixture of vibrationally excited molecules
$c_{pv,s}$	=	specific heat of molecular species s at constant pressure for vibrational excitation
$c_{vel,s}$	=	specific heat of species s at constant volume for electronic excitation
$c_{vv,s}$	=	specific heat of species s at constant volume for vibrational excitation
D_s	=	effective diffusion coefficient of species s
D_{sr}	=	binary diffusion coefficient for s-r species
D_s^a	=	ambipolar diffusion coefficient of ionic species s
D_s^v	=	average vibrational energy per unit mass of molecular species s, which is created or destroyed at rate $\dot{w}_s$
e	=	mixture energy per unit mass
e_{el}	=	mixture electronic energy per unit mass
$e_{el,s}$	=	electronic energy per unit mass of species s
e_s	=	energy per unit mass of species s
e_s^0	=	energy of formation of species s
e_v	=	mixture vibrational energy per unit mass

$e_{v,s}$	=	vibrational energy per unit mass of species s
$e^*_{v,s}$	=	equilibrium vibrational energy per unit mass of species s at translational temperature T
$E_{i,s}$	=	first ionization energy of species s per mole
f	=	scalar quantity
g	=	determinant of general metric tensor
$\underline{g}_i$, $\underline{g}^i$	=	covariant and contravariant general base vectors
g_{ij}, g^{ij}	=	covariant and contravariant general metric tensor components
h	=	mixture enthalpy per unit mass
h_{el}	=	mixture electronic enthalpy per unit mass
$h_{el,s}$	=	electronic enthalpy per unit mass of species s
h_s	=	enthalpy per unit mass of species s
h^0_s	=	heat of formation of species s
h_v	=	mixture vibrational enthalpy per unit mass
$h_{v,s}$	=	vibrational enthalpy per unit mass of species s
J	=	Jacobian of transformation
k	=	Boltzmann constant
$k_{b,p}$	=	backward reaction rate coefficient for reaction p
$k_{f,p}$	=	forward reaction rate coefficient for reaction p
$K_{e,p}$	=	equilibrium constant for reaction p
L	=	body length
Le_s	=	Lewis number of species s
$Le_{v,s}$	=	Lewis number of vibrationally excited molecular species s
m	=	mixture mass
m_s	=	mass of species s
M_s	=	molecular weight of species s
M_∞	=	freestream Mach number, or mixture molecular weight at freestream
$\dot{n}_{e,s}$	=	molar rate of production of ionized species s per unit volume by electron-impact ionization
p	=	pressure
Pr	=	Prandtl number
Pr_v	=	Prandtl number for mixture of vibrationally excited molecules
$\underline{q}$	=	heat-flux vector
q_w	=	wall heat-transfer rate
R	=	ordinary gas constant

$\Re$	=	universal gas constant
Re	=	Reynolds number
S_s	=	bridging function in vibrational rate equation
T	=	translational-rotational temperature of heavy particle
T_a	=	geometrically averaged temperature for dissociative reactions
T_{sh}	=	post-shock translational-rotational temperature
T_v	=	vibrational-electronic-electron temperature
$T_{v,sh}$	=	post-shock vibrational temperature
T_{ij}, T^{ij}	=	covariant and contravariant stress tensor component
T_{ref}	=	reference temperature
U_∞	=	freestream velocity
u, v, w	=	Cartesian velocity components
U, V, W	=	contravariant velocity components in a curvilinear system
$\dot{w}_s$	=	mass production rate of species s per unit volume
$\underline{v}$	=	velocity vector
v^i	=	ith component of velocity
$\underline{V}_s$	=	diffusion velocity vector of species s
x, y, z	=	Cartesian coordinates
x^i	=	general non-orthogonal coordinate
$y^{i'}$	=	Cartesian reference coordinate
y_s	=	molar fraction of species s
$\alpha^i_{i'}$	=	component of contravariant base vector
$\beta^{i'}_i$	=	component of covariant base vector
γ_s	=	molar concentration of species s per unit mass
γ_t	=	total molar concentration of mixture
Γ^j_{ki}	=	Christoffel symbols of the second kind
δ	=	boundary-layer thickness
δ_1	=	mass flow displacement thickness
δ^i_j	=	Kronecker tensor
$\Delta^{(1)}_{sr}$, $\Delta^{(2)}_{sr}$	=	modified collision integrals for the collision pair $s-r$
θ_s	=	characteristic energy for diffusion model for molecular species s
κ_h	=	frozen thermal conductivity for translational-rotational energy of heavy particles

κ_e	=	frozen thermal conductivity of electrons owing to collisions between electrons and all particles
κ_e'	=	frozen thermal conductivity of electrons owing to collisions among electrons
κ_r	=	thermal conductivity for rotational energy
κ_t	=	frozen thermal conductivity for translational energy
κ_v	=	thermal conductivity of vibrational energy owing to collisions between molecules and all particles
κ_v'	=	thermal conductivity of vibrational energy owing to collisions among molecules
λ	=	second coefficient of viscosity
μ	=	viscosity coefficient of mixture
μ_{ref}	=	reference viscosity
ξ, η, ζ	=	curvilinear surface-oriented coordinates
ρ	=	mixture mass density
ρ_e	=	mass density of electrons
ρ_M	=	overall mass density of molecules
ρ_s	=	mass density of species s
σ_v	=	limiting collision cross-section
τ_{cs}	=	collision limited vibrational relaxation time for molecular species s
τ_s	=	combined vibrational relaxation time of molecular species s
$< \tau_s >$	=	average vibrational relaxation time for species s
τ_{sr}	=	vibrational relaxation time for species s with collision partner r
Φ	=	dissipation function
χ	=	transformed normal coordinate, $(= \zeta/\delta)$

Subscripts

e	=	electron
ed	=	boundary-layer outer edge
el	=	electronic excitation mode
i	=	index of the nodes in x^i direction
j	=	index of the nodes in x^j direction
k	=	index of the nodes in x^k direction
r	=	species r, or rotational mode
ref	=	dimensional reference quantity
s	=	species s, or stagnation point; $1 = N$, $2 = O$, $3 = N_2$, $4 = O_2$, $5 = NO$, $6 = N^+$, $7 = O^+$, $8 = N_2^+$, $9 = O_2^+$, $10 = NO^+$, $11 = e^-$
sh	=	post-shock condition
v	=	vibrational mode
w	=	quantity at the wall
∞	=	freestream quantity

Superscripts

$-$	=	dimensional quantity
$*$	=	physical quantity

Conventions

Latin indices in tensor relationships vary between 1 and 3, Greek indices between 1 and 2.

1. Introduction

With the rapid advent of computer hardware and numerical algorithms in the last decade, it is now possible to solve the Navier-Stokes (N-S) equations to simulate the hypersonic flow field around general body configuration with high accuracy [1, 2].

It is extremely difficult, if not impossible, to reproduce experimentally the complex flow fields around present and future space vehicles, such as the Space Shuttle Orbiter, assured crew return vehicle (ACRV), and aeroassisted space transfer vehicle (ASTV), in a ground-based simulation facility. Thus, it becomes highly desirable to rely on computational-fluid-dynamics (CFD) for hypersonic flow simulation. However, systematic application of the N-S solvers to the design of the space vehicles is still limited by the extremely high costs of numerical operation. This is especially true for solving the three-dimensional flow field around a complete geometry, which needs prohibitive amounts of computer time and storage.

Numerical tools for design environments require fast solution of many cases. Presently available three-dimensional methods such as a streamline code and an axisymmetric analog code [3, 4] are too approximate and too restrictive for general use. Furthermore, these codes can not account for real gas effects or surface effects which are important aspects of the hypersonic flight regimes. Consequently, there is a need to develop a computational code which is economical to use and has the required accuracy as an engineering design tool. An attractive candidate for meeting this requirement is the viscous-inviscid two layer approach. By matching the boundary-layer flow to the external inviscid flow about three-dimensional configurations, an entire flow field can be predicted with substantial reduction of the computational effort.

Until the mid 70's, study of three-dimensional compressible boundary-layer theory had been actively conducted [5-8] in the U.S. in relation to the development of hypersonic aircraft. Although these three-dimensional studies were extensive and involved laminar, transitional, and turbulent boundary-layer flows, all of them were based on classical, first-order boundary layer theory. As a result, practical application was limited to smooth bodies like conical geometries and thin wing configurations. In addition, most methods utilized an orthogonal curvilinear coordinate system which further

hindered their use for broad application. Meanwhile, research efforts then were shifted to the development of numerical techniques for solving the full Navier-Stokes (FNS), parabolized Navier-Stokes (PNS) and viscous-shock-layer (VSL) equations, leading to the dwindling of boundary-layer approach.

Classical, first-order boundary-layer theory is based on the assumption of very small curvature compared with the boundary-layer thickness. This is not the case for a general three-dimensional geometry. Furthermore, classical boundary-layer theory can not handle second-order effects such as displacement effects which are provoked by the viscous region, entropy and total enthalpy gradient effects, which originate in the inviscid region of the curved bow shock present in supersonic/hypersonic flow, and body curvature effects. The shock wave curvature in the nose region has a strong influence on downstream aerodynamic heating and on the boundary-layer edge properties, which in turn determine the convective heating load of the vehicle [1]. The limitations of the first-order boundary-layer theory can be overcome to a certain extent by considering these second-order effects properly.

Second-order boundary-layer theory was first studied by Van Dyke [9-11], who distinguished the second-order effects. He expanded flow variables asymptotically in powers of the perturbation parameter $Re^{-1/2}$, where Re is a characteristic Reynolds number. This was done separately for the outer inviscid and inner viscous flows. The results are then substituted into the Navier-Stokes equations to obtain the first- and second-order set of equations for each flow region. To obtain the matching conditions where the regions overlap, the variables of the outer flow were represented by an appropriate expansion of its wall values. Van Dyke applied this approach to two-dimensional and axisymmetric flows. Recently, Aupoix et al. [12, 13] have modified the asymptotic expansion approach in such a way that a smooth matching of the inner and outer solutions is ensured. Their so called 'defect' equations include Van Dyke's equations plus terms of higher order. An attempt to extend this approach to three-dimensional flow is under way.

An alternate way to obtain the second-order boundary-layer equations is the order-of-magnitude analysis which has been widely used for deriving the simplified form of the Navier-Stokes equations. In this analysis, the N-S equations are first expressed in dimensionless form by normalizing all flow variables with reference values while all linear dimensions are normalized by

a characteristic length. Each term of the N-S equations is then estimated and those smaller than a prescribed value are dropped from the equation system. In the first-order theory, only terms of order unity are retained leading to the well known classical boundary layer equations. In the second-order theory, terms up to order $Re^{-1/2}$, which is the same as the perturbation parameter defined by Van Dyke [9-11], are retained. This approach is much easier to understand than the perturbation approach, since it follows the orderly simplification of the full Navier-Stokes equations thus allowing the comparison with PNS and VSL equations depending on the level of approximation. Davis and Flügge-Lotz [14] used this order-of magnitude method comprehensively to develop the VSL equations which are the composite equations for the Euler equations and the second-order viscous equations.

It must be noted that the surface curvature effect is customarily distinguished from the other second-order effects such as the displacement effect, the external entropy gradient effect and the external total enthalpy gradient. All these second order effects only affect the matching of the boundary-layer flow with the external flow and thus influence the boundary conditions of either the outer inviscid region or the inner viscous region without directly intervening in the boundary layer equations. The displacement effect can be dealt with by means of either the displacement surface or the equivalent inviscid source distribution. The entropy and total enthalpy gradient effects, which originate in the inviscid flow region, are taken into account through the iterative viscous-inviscid matching process.

On the other hand, the curvature effect is caused exclusively by the shape of the body surface. When the local boundary-layer thickness is not small compared with the smallest radius of curvature of the body surface, which is the case for any practical body geometry, the curvature produces a non-zero pressure gradient across the boundary layer, expressed by the body-normal momentum equation. Moreover, the curvature contributes other terms to the second-order equations and affects the boundary conditions.

In order to predict correctly the flow field about general three-dimensional geometries based on the viscous-inviscid two-layer model, one must have an elaborate second-order boundary-layer solution, an accurate inviscid Euler solution and a rigorous inner-outer matching technique. Using this strategy, Monnoyer [15-17] has calculated the hypersonic three-dimensional laminar flow on general body configurations. His method is a direct extension of

the comprehensive European efforts [18, 19] in the development of higher-order boundary-layer theory. Monnoyer [15] closely followed the order-of-magnitude analysis of Robert [18], who derived the second-order boundary-layer equations from the N-S equations in a curvilinear non-orthogonal coordinate system [20], and modified the evaluation of surface curvature. Monnoyer applied the second-order boundary-layer equations for solving the three-dimensional flow around an ellipsoid at incidence [16], and then, flow past the windward side of the European space shuttle HERMES [17]. Although Monnoyer has dealt with three-dimensional boundary-layer flow quite extensively, only primitive gas models (perfect and equilibrium gas) have been applied so far. Monnoyer's work and other recent papers [21, 22] demonstrate that the inviscid/boundary layer approach can provide flow predictions for cases without separation that are nearly as accurate as Navier-Stokes solutions and are significantly cheaper.

Apart from the European work, an attempt was made to develop the higher-order boundary-layer equations at the NASA Ames Research Center in the late 80's. Panaras [23] derived the second-order boundary-layer equations for three-dimensional compressible flows. The equations were written in a generalized curvilinear coordinate system, and were developed from the Navier-Stokes equations written in tensor notation by means of an order-of-magnitude analysis. The resulting equations are nearly identical with those developed by Monnoyer [15, 16]. Subsequently, Steger et al. [24, 25] modified Panaras's analysis to describe the boundary-layer equations in general body-fitted curvilinear coordinates while retaining the original Cartesian dependent variables. This alternate form of the boundary-layer equations offers several advantages in terms of numerical stability, and the software (gridding, boundary condition routines, etc) developed for many Navier-Stokes schemes can be readily applied. This attractive new formulation of the boundary-layer equations is, however, rather arbitrarily simplified when applied to sample calculations because of concerns about numerical stability. Very limited calculations for a perfect gas have been undertaken so far. Therefore, the general use of this approach remains to be seen.

In the mid 70's, Gershbein [26] in the former U.S.S.R. developed the system of equations for a three-dimensional chemically reacting laminar boundary layer in curvilinear non-orthogonal coordinate system. His set of equations was a direct extension of the three-dimensional boundary-layer equa-

tions derived by Shevelev [27] for a perfect gas, which was based on first-order boundary layer theory. Due to the first-order analysis, Gershbein dealt with only flows past simple smooth blunt bodies such as an ellipsoid and a cylinder with a primitive gas chemistry.

In the hypersonic flight regime, the thermal and chemical characteristics of air in the shock layer of space vehicles are altered in ways that affect the thermodynamic and transport properties, the chemical reaction rates, and the radiation properties. These properties, in turn, influence the characteristics of the flow, the shear stress, and the heat flux. For the next generation of aerospace vehicles, which usually will fly through the upper atmosphere of Earth, nonequilibrium aerothermochemistry and finite-rate surface catalysis will play an important role in determining the aerodynamic/aerothermodynamic loads to the surface [28-32].

Highly sophisticated high-temperature thermochemical gas models have been developed in recent years at the NASA Ames Research Center [33]. These real gas models have been evolved for the purpose of maturing the enabling technology necessary for the design of proposed aerobraking and aeromaneuvering space vehicle configurations such as an aeroassisted orbital transfer vehicle (AOTV) and transatmospheric vehicle (TAV). The remaining task, therefore, is how to simplify, without significant compromise, these rather complicated thermochemical gas models and to implement them into the engineering flow field solver such as the boundary-layer method.

Since the type of the boundary-layer equations is a parabolic, they can be solved using space-marching integration methods. The Navier-Stokes equations, on the other hand, have to be integrated with time-marching methods which require enormous amounts of computational time and storage. Numerical schemes for the boundary-layer equations are relatively well-established and tested as compared to methods for the other viscous flow equations [34].

The purpose of the present study is to derive the second-order hypersonic three-dimensional thermochemical nonequilibrium boundary-layer equations in generalized curvilinear coordinates. The resulting set of equations will be suitable for the development of a boundary-layer code which allows simultaneous handling of both general three-dimensional configurations and general thermochemically nonequilibrium gas models in an engineering context. Although the future options include wall catalysis, ablation, radiative heat

transfer and turbulent flow, major focus is placed on the three-dimensional laminar boundary-layer flow field around practical geometries with real-gas effects. The strong-viscous interactions, such as flow separation or shock boundary-layer interaction, will not be treated here since these problems are beyond the scope of the boundary-layer approach.

2. Governing Equations

2.1 Coordinate System

The selection of a coordinate system to describe the boundary-layer equations over a three-dimensional body is of major importance and can significantly affect the usefulness and applicability of the final computer code [7]. In addition, the boundary-layer approximation is impractical to implement in any system other than a surface-oriented coordinate system. Selection of an orthogonal system may cause a number of inconveniences together with lengthy interpolation procedures [6]. Consequently, the natural choice for the coordinate system of general three-dimensional boundary-layer equations is a surface-oriented non-orthogonal curvilinear coordinate system where two curvilinear coordinates are locally parallel to the surface and a third coordinate is normal to the surface in order to implement a thin boundary-layer assumption. In this coordinate system, surface-normal derivative terms, which play an important role in the boundary-layer equations, can be easily recognized.

The surface-oriented non-orthogonal curvilinear coordinate system has been widely used in the works of European groups [12-20] , in which they named it a surface-oriented *locally monoclinic* coordinate system. They used extensive tensor concepts, which are complicated enough to scare off the unfamiliar reader, to derive the boundary-layer equations and to determine the metric properties of the body surface. Furthermore, their unique use of index notation and so-called 'shifters' may cause unnecessary confusion. On the other hand, Panaras [23] described the system of equations in such a way that the interface between the analytical partial-differentiation notation and the tensor notation is easily understandable. Therefore, the tensor formulation and the order-of-magnitude analysis of Panaras [23] are used in the present study along with the boundary condition treatment, boundary-layer parameters and inner-outer layer matching procedure of the European groups[12-19]. To avoid confusion, however, the usual notation of fluid dynamics is employed with 'minimal' use of tensor expressions.

2.1.1 Base Vectors and Metric Coefficients

The general non-orthogonal, curvilinear surface-oriented coordinate system $x^i(\xi,\eta,\zeta)$ is depicted in Fig. 1 where the Cartesian coordinate system $y^{i'}(x,y,z)$ is used as a reference. The coordinate system consists of two curvilinear coordinates ξ and η locally parallel to the surface and a third coordinate ζ locally orthogonal to the other two coordinates and rectilinear. It must be noted that the complete space above the surface can be uniquely described by these coordinates if the surface is convex but only partly if the surface is concave [15].

In the present paper, only the essential geometric relations, which result from coordinate transformation and which are presented in tensor notation, are described. The detailed tensor analysis applied to the basic equations of fluid dynamics can be found in [15, 19, 20]. In tensor notation, superscripted indices, e.g. u^i, are called contravariant tensors and subscripted indices, e.g. u_i, covariant tensors. In Fig. 1, $\underline{e}_{i'}$ is an unit vector in the Cartesian reference coordinate system, $\underline{a}_i$ is a covariant vector at the surface ($\zeta = 0$) and $\underline{g}_i$ is a general covariant base vector (off-surface points). The general covariant base vector $\underline{g}_i$ in this system is defined by the transformation [20]

$$\underline{g}_i = \frac{\partial y^{i'}}{\partial x^i}\underline{e}_{i'} = \beta_i^{i'}\underline{e}_{i'}; \quad (i,i' = 1,2,3) \tag{1}$$

where the notation $\beta_i^{i'}$ is defined by

$$\beta_i^{i'} \equiv \frac{\partial y^{i'}}{\partial x^i} \tag{2}$$

In the present notation, the Einstein summation convention is used throughout, e.g.:

$$\beta_i^{i'}\underline{e}_{i'} = \beta_i^{1'}\underline{e}_{1'} + \beta_i^{2'}\underline{e}_{2'} + \beta_i^{3'}\underline{e}_{3'}$$

In a general non-orthogonal curvilinear coordinate system, the base vector $\underline{g}_i$ is neither perpendicular nor of unit length contrary to the case for a Cartesian coordinate system.

Similarly, the covariant base vector at the surface is defined by

$$\underline{a}_i = \dot{\beta}_i^{i'}\underline{e}_{i'}; \quad (i,i' = 1,2,3) \tag{3}$$

where the superscript '$\cdot$' denotes a quantity at a point on the body surface. The contravariant base vector $\underline{g}^i$ is defined by

$$\underline{g}^i = \frac{\partial x^i}{\partial y^{i'}}\underline{e}_{i'} = \alpha_{i'}^i\underline{e}_{i'}; \quad (i,i' = 1,2,3) \tag{4}$$

where $\alpha^i_{i'}$ is defined by

$$\alpha^i_{i'} \equiv \frac{\partial x^i}{\partial y^{i'}} \tag{5}$$

The contravariant base vector must satisfy the relation

$$\underline{g}^k \cdot \underline{g}_i = \delta^k_i \tag{6}$$

where δ^k_i is the Kronecker tensor

$$\delta^k_i = \begin{bmatrix} 1 & 0 & 0 \\ 0 & 1 & 0 \\ 0 & 0 & 1 \end{bmatrix}$$

It must be noted that in a Cartesian coordinate system the covariant and the contravariant base are identical.
The covariant metric tensor components g_{ij} is defined by

$$g_{ij} = \underline{g}_i \cdot \underline{g}_j = \sum_{i'=1}^{3} \beta^{i'}_i \beta^{i'}_j \tag{7}$$

The contravariant metric tensor components g^{il} are given by the orthogonality relation

$$g_{ij} g^{il} = \delta^l_j \tag{8}$$

thus, they are connected to the components of the covariant metric tensor with the relation

$$g^{il} = \frac{1}{g}(g_{jm} g_{kn} - g_{jn} g_{km}) \tag{9}$$

where indices (i, j, k) and (l, m, n) are cyclic.
Here, g is the determinant of the metric tensor

$$g \equiv |g_{ij}| \equiv \begin{vmatrix} g_{11} & g_{12} & g_{13} \\ g_{21} & g_{22} & g_{23} \\ g_{31} & g_{32} & g_{33} \end{vmatrix} = \frac{1}{|g^{il}|}$$

Therefore, the Jacobian of the transformation from $y^{i'}(x, y, z)$ to $x^i(\xi, \eta.\zeta)$

$$J \equiv \frac{\partial(\xi.\eta, \zeta)}{\partial(x, y, z)} = \begin{vmatrix} \xi_x & \xi_y & \xi_z \\ \eta_x & \eta_y & \eta_z \\ \zeta_x & \zeta_y & \zeta_z \end{vmatrix} = |\alpha^i_{i'}|$$

is related to the determinant g by the relation

$$J = \frac{1}{\sqrt{g}} \tag{10}$$

When differentiating tensors in terms of curvilinear coordinates, certain combinations of partial derivatives of metric tensor components (the Christoffel symbols) play an important role. The Christoffel symbols of the second kind are defined by

$$\Gamma_{ij}^{k} = \Gamma_{ji}^{k} = \frac{\partial \underline{g}_i}{\partial x^j} \cdot \underline{g}^k \tag{11}$$

Γ_{ij}^{k} are further denoted by

$$\Gamma_{ij}^{k} = \frac{1}{2} g^{lk} \left(\frac{\partial g_{jl}}{\partial x^i} + \frac{\partial g_{il}}{\partial x^j} - \frac{\partial g_{ij}}{\partial x^l} \right) \tag{12}$$

The Christoffel symbols may be interpreted in terms of the variation of base vectors with respect to the coordinates. The Christoffel symbols are zero in a Cartesian coordinates system.
In the present coordinate system, the base vectors $\underline{g}_i$ are space-dependent and $\underline{g}_3$ is an unit vector, thus g_{ij} takes the form:

$$g_{ij} = \begin{bmatrix} g_{11} & g_{12} & 0 \\ g_{12} & g_{22} & 0 \\ 0 & 0 & 1 \end{bmatrix}$$

and the determinant g of the metric tensor becomes

$$g \equiv g_{11} g_{22} - (g_{12})^2 \tag{13}$$

where the off-diagonal term g_{12} equals zero for orthogonal coordinates. For explicit expression of the metric tensor components, see Appendix A.
The metric tensor at the surface is a special case of g_{ij} [19]:

$$a_{\alpha\beta}(x^\alpha) = g_{ij}(x^\alpha, x^3 = 0); \quad (\alpha, \beta = 1, 2) \tag{14}$$

thus, the surface metric tensor becomes

$$a_{\alpha\beta} = \begin{bmatrix} a_{11} & a_{12} \\ a_{12} & a_{22} \end{bmatrix}$$

The covariant curvature tensor $b_{\alpha\beta}$ of the surface is defined by [19]

$$b_{\alpha\beta} = \frac{\partial \underline{a}_\alpha}{\partial x^\beta} \cdot \underline{a}_3; \quad (\alpha, \beta = 1, 2) \tag{15}$$

With equation(3), $b_{\alpha\beta}$ can be expressed by

$$b_{\alpha\beta} = \sum_{k'=1}^{3} \frac{\partial \dot{\beta}_\alpha^{k'}}{\partial x^\beta} \dot{\beta}_3^{k'} = \begin{bmatrix} b_{11} & b_{12} \\ b_{12} & b_{22} \end{bmatrix}$$

Similar simplifications can be applied to the Christoffel symbols.

$$\Gamma_{3\alpha}^3 = \Gamma_{\alpha 3}^3 = \Gamma_{33}^\alpha = \Gamma_{33}^3 = 0 \quad (\alpha = 1, 2) \tag{16}$$

Equation (16) states that any Christoffel symbol vanishes if more than one of its indices is a 3 (normal coordinate). For details, see Appendix B.

2.1.2 Physical Flow Quantity

In non-Cartesian coordinate systems, in general, tensor components do not have the correct physical dimension even if they are orthogonal. This is due to the fact that in such coordinate frames the base vectors are functions of the coordinates x^i and are not necessarily dimensionless unit vectors as in a Cartesian system [20, 35]. Any vector $\underline{v}$ can be written as the sum of its components with respect to an arbitrary set of covariant (contravariant) base vectors $\underline{g}_i(\underline{g}^i)$ referred to a particular point in space:

$$\underline{v} = v^i \underline{g}_i = v_i \underline{g}^i \tag{17}$$

where v^i is a contravariant velocity component and v_i is a covariant velocity component.
The contravariant *physical* velocity component v^{*i} is defined by

$$\underline{v} = v^{*i} \underline{e}_i \tag{18}$$

where $\underline{e}_i$ is an unit vector parallel to the covariant base vector $\underline{g}_i$. Since

$$\underline{e}_i = \frac{\underline{g}_i}{\sqrt{\underline{g}_i \cdot \underline{g}_i}} = \frac{\underline{g}_i}{\sqrt{g_{ii}}} \tag{19}$$

Then

$$v^{*i} = \sqrt{g_{ii}} v^i \tag{20}$$

In similar fashion, the covariant *physical* velocity component v_i^* is given by

$$v_i^* = \sqrt{g^{ii}} v_i \tag{21}$$

2.1.3 Covariant Derivatives

When differentiating a vector in terms of curvilinear coordinates, not only the vector itself but also the corresponding base vectors have to be differentiated as well since they are space-dependent.
The partial derivative of a vector $\underline{v}$ consists of two parts [20]:

$$\begin{aligned} \frac{\partial \underline{v}}{\partial x^j} &= \frac{\partial v^i}{\partial x^j} \underline{g_i} + v^i \frac{\partial \underline{g_i}}{\partial x^j} \\ &= \left(\frac{\partial v^i}{\partial x^j} + \Gamma^i_{jk} v^k\right) \underline{g_i} \end{aligned} \tag{22}$$

wherein

$$v^i|_j \equiv \frac{\partial v^i}{\partial x^j} + \Gamma^i_{jk} v^k \tag{23}$$

is called the covariant derivative of the contravariant vector component v^i.
The covariant derivative of stress tensor component T^{ij} is given by the relation:

$$T^{ij}|_k \equiv \frac{\partial T^{ij}}{\partial x^k} + \Gamma^i_{kl} T^{lj} + \Gamma^j_{kl} T^{il} \tag{24}$$

In the case of a scalar f, the covariant derivative reduces to the partial derivative with respect to the coordinate

$$f|_j = \frac{\partial f}{\partial x^j} \tag{25}$$

The divergence of a vector $\underline{A}$ is defined by [23]

$$div \underline{A} \equiv \frac{\partial A^i}{\partial x^i} + \Gamma^i_{ij} A^j \tag{26}$$

Since

$$\Gamma^i_{ij} = \frac{1}{\sqrt{g}} \frac{\partial}{\partial x^i}(\sqrt{g}) \tag{27}$$

$$div \underline{A} = \frac{1}{\sqrt{g}} \frac{\partial}{\partial x^i}(A^i \sqrt{g}) = \frac{1}{\sqrt{g}} \frac{\partial}{\partial x^i}(g^{ij} A_j \sqrt{g}) \tag{28}$$

Similarly

$$T^{ij}|_j = \frac{1}{\sqrt{g}} \frac{\partial}{\partial x^l}(T^{il} \sqrt{g}) + \Gamma^i_{lj} T^{lj} \tag{29}$$

2.2 Dimensional Form of the Navier-Stokes Equations

In the present paper, we deal with thermal and chemical nonequilibrium air flow with 11 species (N, O, N_2, O_2, NO, N^+, O^+, N_2^+, O_2^+, NO^+, e^-). To reduce the complexity of the general three-temperature thermal model developed by Lee [29], the two-temperature approach proposed by Park [36, 37] is adopted in the present study. For the details of general basic equations based on the three-temperature model for hypersonic thermochemical nonequilibrium flow in Cartesian coordinates, see Ref. 29. According to Park's two-temperature model [36, 37], translational-rotational temperature T and vibrational-electronic-electron temperature T_v are necessary to describe the system of governing equations and to express the chemical reaction rates and thermodynamic and transport properties. The concept of a two-temperature model originates in the fact that the energy transfer rate between the translational mode of free electrons and the vibrational mode of molecular nitrogen (e-V process) is much faster than the rate between translational and vibrational modes of nitrogen molecules (T-V process) [38, 39].

The necessary set of basic governing equations consists of overall mass, overall momentum, vibrational-electronic-electron energy, overall energy and species mass conservation equations plus the complementary equations of state, which are required to close the system of equations. In deriving the equations, diffusion due to the species concentration gradient is considered, while thermal and pressure diffusion are neglected.

The dimensional form of the Navier-Stokes equations for steady thermochemical nonequilibrium flow written in general curvilinear coordinates system $\overline{x}^i$ are given by [20, 23, 29, 40]

Continuity:

$$\frac{\partial}{\partial \overline{x}^i}(\overline{\rho v}^i \sqrt{g}) = 0 \tag{30}$$

Momentum:

$$\overline{\rho v}^j \frac{\partial \overline{v}^i}{\partial \overline{x}^j} + \overline{\rho}\overline{\Gamma}^i_{jk}\overline{v}^j\overline{v}^k = \overline{T}^{ij}|_j \tag{31}$$

where the stress tensor $\overline{T}^{ij}$ and its covariant derivative $\overline{T}^{ij}|_j$ are given by

$$\overline{T}^{ij} = (-\overline{p} + \overline{\lambda}\overline{v}^k|_k)g^{ij} + \overline{\mu}(g^{im}\overline{v}^j|_m + g^{jn}\overline{v}^i|_n) \tag{32}$$

$$\begin{aligned}
\overline{T}^{ij}|_j &= \frac{1}{\sqrt{g}}\frac{1}{\partial \overline{x}^j}(\overline{T}^{ij}\sqrt{g}) + \overline{\Gamma}^i_{jk}\overline{T}^{jk} \\
&= g^{ij}\frac{\partial}{\partial \overline{x}^j}[-\overline{p} + \overline{\lambda}\frac{1}{\sqrt{g}}\frac{\partial}{\partial \overline{x}^k}(\overline{v}^k\sqrt{g})] \\
&+ \frac{1}{\sqrt{g}}\frac{\partial}{\partial \overline{x}^j}[\overline{\mu}\sqrt{g}(g^{im}\overline{v}^j|_m + g^{jn}\overline{v}^i|_n)] \\
&+ \overline{\Gamma}^i_{jk}\overline{\mu}(g^{jm}\overline{v}^k|_m + g^{kn}\overline{v}^j|_n)
\end{aligned} \tag{33}$$

Vibrational-electronic-electron energy:

$$\begin{aligned}
\overline{\rho v}^i \frac{\partial \overline{e}_V}{\partial \overline{x}^i} &= -\overline{p}_e(\frac{\partial \overline{v}^i}{\partial \overline{x}^j} + \overline{\Gamma}^i_{jk}\overline{v}^k) + \frac{1}{\sqrt{g}}\frac{\partial}{\partial \overline{x}^j}[\sqrt{g}(\overline{\kappa}'_v + \overline{\kappa}_e)g^{ij}\frac{\partial \overline{T}_v}{\partial \overline{x}^j}] \\
&+ \frac{1}{\sqrt{g}}\frac{\partial}{\partial \overline{x}^j}[\sqrt{g}\overline{\rho}\sum_{s=1}^{11}\overline{h}_{V,s}\overline{D}_s g^{ij}\frac{\partial C_s}{\partial \overline{x}^j}] \\
&+ \overline{\rho}\sum_{s=M} C_s\frac{\overline{e}^*_{v,s} - \overline{e}_{v,s}}{\overline{\tau}_s}|\frac{\overline{T}_{sh} - \overline{T}_v}{\overline{T}_{sh} - \overline{T}_{v,sh}}|^{S_s} \\
&+ 3\overline{\rho}_e\overline{\Re}(\overline{T} - \overline{T}_v)\sum_{r=1}^{10}\frac{\overline{\nu}^*_{er}}{\overline{M}_r} - \sum_{s=6}^{10}\overline{n}_{e,s}\overline{E}_{i,s} + \sum_{s=M}\overline{w}_s\overline{D}^v_s
\end{aligned} \tag{34}$$

Overall energy:

$$\overline{\rho v^i}\frac{\partial \overline{h}}{\partial \overline{x^i}} - \overline{v^i}\frac{\partial \overline{p}}{\partial \overline{x^i}} = \overline{\Phi} + \frac{1}{\sqrt{g}}\frac{\partial}{\partial \overline{x^i}}(\sqrt{g}\overline{\kappa}_h g^{ij}\frac{\partial \overline{T}}{\partial \overline{x^j}})$$
$$+ \frac{1}{\sqrt{g}}\frac{\partial}{\partial \overline{x^i}}[\sqrt{g}(\overline{\kappa}_v + \overline{\kappa}_e)g^{ij}\frac{\partial \overline{T}_v}{\partial \overline{x^j}}] + \frac{1}{\sqrt{g}}\frac{\partial}{\partial \overline{x^i}}(\sqrt{g\rho}\sum_{s=1}^{11}\overline{h}_s\overline{D}_s g^{ij}\frac{\partial C_s}{\partial \overline{x^j}}) \quad (35)$$

where the dissipation function is given by

$$\overline{\Phi} = \overline{\lambda}\overline{v^i}|_i\overline{v^l}|_l + \overline{\mu}\frac{\partial}{\partial \overline{x^i}}[(g^{im}\overline{v^j}|_m + g^{jn}\overline{v^i}|_n)g_{jk}\overline{v^k}] \quad (36)$$

Species continuity:

$$\overline{\rho v^i}\frac{\partial C_s}{\partial \overline{x^i}} = \frac{1}{\sqrt{g}}\frac{\partial}{\partial \overline{x^i}}(\overline{\rho}\overline{D}_s\frac{\partial C_s}{\partial \overline{x^i}}) + \overline{\dot{w}_s}; \quad (s = 1, 2, \ldots, 11) \quad (37)$$

Equation of state:

$$\overline{p} = \overline{\Re}\overline{\rho}(\sum_{s=1}^{10} C_s\frac{\overline{T}}{\overline{M}_s} + C_e\frac{\overline{T}_v}{\overline{M}_e}) \quad (38)$$

Equation of state for electrons:

$$\overline{p}_e = \overline{\Re}\overline{\rho}C_e\frac{\overline{T}_v}{\overline{M}_e} \quad (39)$$

In the above equations system, an overbar '-' denotes a dimensional quantity.

The heat-flux vector $\overline{q^i}$, in tensor notation, can be expressed as

$$\overline{q^i} = -\overline{\kappa}_h g^{ij}\frac{\partial \overline{T}}{\partial \overline{x^i}} - (\overline{\kappa}_v + \overline{\kappa}_e)g^{ij}\frac{\partial \overline{T}_v}{\partial \overline{x^i}} - \overline{\rho}\sum_{s=1}^{11}\overline{h}_s\overline{D}_s g^{ij}\frac{\partial C_s}{\partial \overline{x^i}} \quad (40)$$

2.3 Normalized Form of the Boundary-Layer Equations

The second-order boundary-layer equations are derived in a system of coordinates where the surface coordinates are denoted by $(\overline{x}^1, \overline{x}^2) = (\overline{\xi}, \overline{\eta})$, and

the normal one by $\overline{x}^3 = \overline{\zeta}$. In order to carry out the order-of-magnitude analysis, the independent variables $\overline{\xi}$, $\overline{\eta}$, $\overline{\zeta}$ and the flow variables are normalized as follows:

$$\xi = \frac{\overline{\xi}}{\overline{L}_{ref}}, \qquad \eta = \frac{\overline{\eta}}{\overline{L}_{ref}}, \qquad \zeta = \frac{\overline{\zeta}}{\overline{L}_{ref}}$$

$$U = \frac{\overline{U}}{\overline{U}_\infty}, \qquad V = \frac{\overline{V}}{\overline{U}_\infty}, \qquad W = \frac{\overline{W}}{\overline{U}_\infty}$$

$$\rho = \frac{\overline{\rho}}{\overline{\rho}_\infty}, \qquad \rho_e = \frac{\overline{\rho}_e}{\overline{\rho}_\infty}, \qquad p = \frac{\overline{p}}{\overline{\rho}_\infty \overline{U}_\infty^2}$$

$$p_e = \frac{\overline{p}_e}{\overline{\rho}_\infty \overline{U}_\infty^2}, \qquad T = \frac{\overline{T}}{\overline{T}_{ref}}, \qquad T_v = \frac{\overline{T}_v}{\overline{T}_{ref}}$$

$$e_V = \frac{\overline{e}_V}{\overline{U}_\infty^2}, \qquad e_{v,s} = \frac{\overline{e}_{v,s}}{\overline{U}_\infty^2}, \qquad h_s = \frac{\overline{h}_s}{\overline{U}_\infty^2}$$

$$h_{V,s} = \frac{\overline{h}_{V,s}}{\overline{U}_\infty^2}, \qquad c_{p,s} = \frac{\overline{c}_{p,s}}{\overline{c}_{p\infty}}, \qquad \mu = \frac{\overline{\mu}}{\overline{\mu}_{ref}}$$

$$\lambda = \frac{\overline{\lambda}}{\overline{\mu}_{ref}}, \qquad \kappa_h = \frac{\overline{\kappa}_h}{\overline{\mu}_{ref}\overline{c}_{p\infty}}, \qquad \kappa_v = \frac{\overline{\kappa}_v}{\overline{\mu}_{ref}\overline{c}_{p\infty}}$$

$$\kappa_v' = \frac{\overline{\kappa}_v'}{\overline{\mu}_{ref}\overline{c}_{p\infty}}, \qquad \kappa_e = \frac{\overline{\kappa}_e}{\overline{\mu}_{ref}\overline{c}_{p\infty}}, \qquad \kappa_e' = \frac{\overline{\kappa}_e'}{\overline{\mu}_{ref}\overline{c}_{p\infty}}$$

$$\dot{w}_s = \frac{\overline{\dot{w}}_s \overline{L}_{ref}}{\overline{\rho}_\infty \overline{U}_\infty}, \qquad \dot{n}_{e,s} = \frac{\overline{\dot{n}}_{e,s}\overline{L}_{ref}\overline{M}_\infty}{\overline{\rho}_\infty \overline{U}_\infty}, \qquad D_s^v = \frac{\overline{D}_s^v}{\overline{U}_\infty^2}$$

$$E_{i,s} = \frac{\overline{E}_{i,s}}{\overline{M}_\infty \overline{U}_\infty^2}, \qquad \tau_s = \frac{\overline{\tau}\overline{U}_\infty}{\overline{L}_{ref}}, \qquad \nu_{er}^* = \frac{\overline{\nu}_{er}^* \overline{L}_{ref}}{\overline{U}_\infty}$$

$$q_w = \frac{\overline{q}_w \overline{L}_{ref}}{\overline{\mu}_{ref}\overline{U}_\infty^2}$$

where the overbar '-' indicates dimensional quantities, subscript 'ref' reference quantities and '∞' freestream quantities.

In the above equations, the velocity vector components U, V and W are the contravariant velocity components, which are connected to the Cartesian velocity components u, v and w by the components of the contravariant base

vectors

$$U = \xi_x u + \xi_y v + \xi_z w$$

$$V = \eta_x u + \eta_y v + \eta_z w$$

$$W = \zeta_x u + \zeta_y v + \zeta_z w \tag{41}$$

Furthermore, they are related to the physical contravariant velocity components U^*, V^* and W^* by means of the diagonal elements of the metric tensor g_{ij} [equation(20)].

$$U = \frac{U^*}{\sqrt{g_{11}}}, \quad V = \frac{V^*}{\sqrt{g_{22}}} \tag{42}$$

and since $g_{33} = 1$,

$$W = W^* \tag{43}$$

On the other hand, the derivative of a scalar quantity such as the pressure is related to the Cartesian pressure derivatives by the chain-rule [23]

$$p_\xi = x_\xi p_x + y_\xi p_y + z_\xi p_z$$

$$p_\eta = x_\eta p_x + y_\eta p_y + z_\eta p_z$$

$$p_\zeta = x_\zeta p_x + y_\zeta p_y + z_\zeta p_z \tag{44}$$

The second-order, three-dimensional, compressible boundary-layer equations have been derived previously from the non-dimensional Navier-Stokes equations by an order-of-magnitude analysis in non-orthogonal locally normal surface-oriented coordinate system [15-18,23]. In addition to the boundary-layer thickness parameter δ, which is the order of $\mathrm{Re}^{-1/2}$, Monnoyer [15] introduced the following curvature parameter k:

$$k = max(\mid K_1 \mid, \mid K_2 \mid) \tag{45}$$

where K_1 and K_2 are the principal curvatures of the surface (see Appendix C). According to Monnoyer's analysis, first-order theory is applied when $O(k) \leq O(1)$, which is equivalent to the classical boundary-layer assumption $O(1/k) \gg O(\delta)$ which states the local radius of curvature of the surface is much larger than the boundary-layer thickness. In this case, the variation of the metric coefficients across the boundary layer is negligible. On the

other hand, if $O(1) < O(k) \leq O(1/\delta)$, then the variation of the metric coefficients with distance from the surface is no longer negligible, and the second-order terms must be considered. This second-order condition of Monnoyer is equivalent to the one in Panaras' analysis that the normal derivatives of the metrics are assumed to be $O(1) < \partial g_{ij}/\partial x^3 \leq O(1/\delta), (i,j = 1,2)$ for large surface-curvature [23]. As mentioned in 2.1, the order-of-magnitude analysis of Panaras is used here mainly because of its simplicity along with the methods of the European groups for boundary conditions, boundary-layer parameters and inner-outer layer matching [12-19].

The order-of-magnitude analysis of Panaras is applied to the system of basic governing equations (30)-(37). The resulting second-order, three-dimensional, laminar boundary-layer equations for a multicomponent two-temperature chemically reacting gas mixture in the curvilinear coordinate system (ξ, η, ζ) are given by

Continuity:

$$\frac{\partial(\rho U\sqrt{g})}{\partial\xi} + \frac{\partial(\rho V\sqrt{g})}{\partial\eta} + \frac{\partial(\rho W\sqrt{g})}{\partial\zeta} = 0 \tag{46}$$

ξ-momentum:

$$\begin{aligned}
&\rho U\frac{\partial U}{\partial\xi} + \rho V\frac{\partial U}{\partial\eta} + \rho W\frac{\partial U}{\partial\zeta} + \rho U^2\Gamma^1_{11} + 2\rho UV\Gamma^1_{12} + \rho V^2\Gamma^1_{22} \\
&\quad = -\frac{g_{22}}{g}\frac{\partial p}{\partial\xi} + \frac{g_{12}}{g}\frac{\partial p}{\partial\eta} \\
&\quad + \frac{1}{Re}\frac{\partial}{\partial\zeta}(\mu\frac{\partial U}{\partial\zeta}) + \underline{\frac{1}{Re}\frac{1}{\sqrt{g}}\mu\frac{\partial U}{\partial\zeta}\frac{\partial\sqrt{g}}{\partial\zeta}} \\
&\quad + \underline{\frac{1}{Re}\frac{1}{\sqrt{g}}\frac{\partial}{\partial\zeta}[\sqrt{g}\mu(U\Gamma^1_{31} + V\Gamma^1_{23})]} + \underline{\frac{\mu}{Re}\frac{\partial U}{\partial\zeta}\Gamma^1_{31}} + \underline{\frac{\mu}{Re}\frac{\partial V}{\partial\zeta}\Gamma^1_{23}}
\end{aligned} \tag{47}$$

η-momentum:

$$\begin{aligned}
&\rho U\frac{\partial V}{\partial\xi} + \rho V\frac{\partial V}{\partial\eta} + \rho W\frac{\partial V}{\partial\zeta} + \rho U^2\Gamma^2_{11} + 2\rho UV\Gamma^2_{12} + \rho V^2\Gamma^2_{22} \\
&\quad = \frac{g_{12}}{g}\frac{\partial p}{\partial\xi} - \frac{g_{11}}{g}\frac{\partial p}{\partial\eta} \\
&\quad + \frac{1}{Re}\frac{\partial}{\partial\zeta}(\mu\frac{\partial V}{\partial\zeta}) + \underline{\frac{1}{Re}\frac{1}{\sqrt{g}}\mu\frac{\partial V}{\partial\zeta}\frac{\partial\sqrt{g}}{\partial\zeta}}
\end{aligned}$$

$$+\underline{\frac{1}{Re}\frac{1}{\sqrt{g}}\frac{\partial}{\partial\zeta}[\sqrt{g}\mu(U\Gamma_{31}^2+V\Gamma_{23}^2)]}+\underline{\frac{\mu}{Re}\frac{\partial U}{\partial\zeta}\Gamma_{31}^2}+\underline{\frac{\mu}{Re}\frac{\partial V}{\partial\zeta}\Gamma_{23}^2} \quad (48)$$

ζ-momentum:

$$\underline{\frac{1}{2}\rho U^2\frac{\partial g_{11}}{\partial\zeta}}+\underline{\rho UV\frac{\partial g_{12}}{\partial\zeta}}+\underline{\frac{1}{2}\rho V^2\frac{\partial g_{22}}{\partial\zeta}}=-\frac{\partial p}{\partial\zeta} \quad (49)$$

Vibrational-electronic-electron energy:

$$\begin{aligned}
&\rho U\frac{\partial e_V}{\partial\xi}+\rho V\frac{\partial e_V}{\partial\eta}+\rho W\frac{\partial e_V}{\partial\zeta}=p_e[\frac{\partial W}{\partial\zeta}\\
&\quad+(\Gamma_{11}^1+\Gamma_{11}^2)U+(\Gamma_{12}^1+\Gamma_{12}^2)(U+V)+(\Gamma_{22}^1+\Gamma_{22}^2)V]\\
&\quad+\frac{1}{Re}\frac{\partial}{\partial\zeta}[(\kappa_v'+\kappa_e)\frac{\partial T_v}{\partial\zeta}]+\underline{\frac{1}{Re}\frac{\partial}{\partial\zeta}\frac{(\kappa_v'+\kappa_e)}{\sqrt{g}}\frac{\partial\sqrt{g}}{\partial\zeta}\frac{\partial T_v}{\partial\zeta}}\\
&\quad+\frac{1}{Re}\frac{\partial}{\partial\zeta}(\sum_{s=1}^{11}\frac{\mu Le_{v,s}}{Pr_v}h_{V,s}\frac{\partial C_s}{\partial\zeta})+\underline{\frac{1}{Re}\frac{1}{\sqrt{g}}\sum_{s=1}^{11}(\frac{\mu Le_{v,s}}{\mathrm{Pr}_v}h_{V,s})\frac{\partial\sqrt{g}}{\partial\zeta}\frac{\partial C_s}{\partial\zeta}}\\
&\quad+\rho\sum_{s=M}C_s\frac{e_{v,s}^*-e_{v,s}}{\tau_s}|\frac{T_{sh}-T_v}{T_{sh}-T_{v,sh}}|^{S_s-1}+3(\frac{\overline{R}}{\overline{c}_{p\infty}})\rho(T-T_v)\sum_{r=1}^{10}\frac{\nu_{er}^*}{M_r}\\
&\quad-\sum_{s=6}^{10}\dot{n}_{e,s}E_{i,s}+\sum_{s=M}\dot{w}_sD_s^v
\end{aligned} \quad (50)$$

Overall energy:

$$\begin{aligned}
&\rho(U\frac{\partial h}{\partial\xi}+V\frac{\partial h}{\partial\eta}+W\frac{\partial h}{\partial\zeta})-(U\frac{\partial p}{\partial\xi}+V\frac{\partial p}{\partial\eta}+W\frac{\partial p}{\partial\zeta})\\
&\quad=\frac{1}{Re}\frac{\partial}{\partial\zeta}(\kappa_h\frac{\partial T}{\partial\zeta})+\frac{1}{Re}\frac{\partial}{\partial\zeta}[(\kappa_v+\kappa_e)\frac{\partial T_v}{\partial\zeta}]\\
&\quad+\underline{\frac{1}{Re}\frac{\kappa_h}{\sqrt{g}}\frac{\partial\sqrt{g}}{\partial\zeta}\frac{\partial T}{\partial\zeta}}+\underline{\frac{1}{Re}\frac{\partial}{\partial\zeta}\frac{(\kappa_v+\kappa_e)}{\sqrt{g}}\frac{\partial\sqrt{g}}{\partial\zeta}\frac{\partial T_v}{\partial\zeta}}\\
&\quad+\frac{\mu}{Re}[g_{11}\frac{\partial}{\partial\zeta}(U\frac{\partial U}{\partial\zeta})+g_{12}\frac{\partial}{\partial\zeta}(V\frac{\partial U}{\partial\zeta})+g_{12}\frac{\partial}{\partial\zeta}(U\frac{\partial V}{\partial\zeta})+g_{22}\frac{\partial}{\partial\zeta}(V\frac{\partial V}{\partial\zeta})]\\
&\quad+\underline{\frac{\mu}{Re}[U\frac{\partial U}{\partial\zeta}\frac{\partial g_{11}}{\partial\zeta}+V\frac{\partial U}{\partial\zeta}\frac{\partial g_{12}}{\partial\zeta}+U\frac{\partial V}{\partial\zeta}\frac{\partial g_{12}}{\partial\zeta}+V\frac{\partial V}{\partial\zeta}\frac{\partial g_{22}}{\partial\zeta}]}\\
&\quad+\frac{1}{Re}\frac{\partial}{\partial\zeta}(\sum_{s=1}^{11}\frac{\mu Le_s}{Pr}h_s\frac{\partial C_s}{\partial\zeta})+\underline{\frac{1}{Re}\frac{1}{\sqrt{g}}\sum_{s=1}^{11}(\frac{\mu Le_s}{Pr}h_s)\frac{\partial\sqrt{g}}{\partial\zeta}\frac{\partial C_s}{\partial\zeta}}
\end{aligned} \quad (51)$$

Species continuity:

$$\rho U\frac{\partial C_s}{\partial \xi}+\rho V\frac{\partial C_s}{\partial \eta}+\rho W\frac{\partial C_s}{\partial \zeta}$$
$$=\frac{1}{Re}\frac{\partial}{\partial \zeta}(\frac{\mu Le_s}{Pr}\frac{\partial C_s}{\partial \zeta})+\underline{\frac{1}{Re}\frac{1}{\sqrt{g}}\frac{\mu Le_s}{Pr}\frac{\partial \sqrt{g}}{\partial \zeta}\frac{\partial C_s}{\partial \zeta}}$$
$$+\dot{w}_s \quad (s=1,2,\ldots,11) \tag{52}$$

The equation of state is

$$p=(\frac{\overline{\Re T}_\infty}{\overline{U}_\infty^2\overline{M}_\infty})\rho(\sum_{s=1}^{10}\frac{C_s}{M_s}T+\frac{C_e}{M_e}T_v) \tag{53}$$

where $\overline{\Re}$ is the universal gas constant, and $\overline{M}_\infty$ is a mixture molecular weight at the freestream.

Similarly the equation of state for electrons is given by

$$p_e=(\frac{\overline{\Re T}_\infty}{\overline{U}_\infty^2\overline{M}_\infty})\rho\frac{C_e}{M_e}T_v \tag{54}$$

In equation (50), e_V is the vibrational-electronic-electron energy of mixture per unit mass, and $h_{V,s}$ is the vibrational-electronic-electron enthalpy for species s per unit mass. These are defined by

$$e_V=e_v+e_{el} \tag{55}$$

$$h_{V,s}=h_{v,s}+h_{el,s} \tag{56}$$

The enthalpy of the mixture, h, is expressed by

$$h=\sum_{s=1}^{11}C_sh_s \tag{57}$$

where h_s is the enthalpy of species s including the heat of formation.

Supplementary relations are given by

$$\sum_{s=1}^{11}C_s=1 \tag{58}$$

$$\sum_{s=1}^{11} \dot{w}_s = 0 \tag{59}$$

The normalized heat-transfer rate to the wall is given by

$$q_w = -\kappa_h \frac{\partial T}{\partial \zeta}|_w - (\kappa_v + \kappa_e)\frac{\partial T_v}{\partial \zeta}|_w - \sum_{s=1}^{11}(\frac{\mu Le_s}{Pr})h_s \frac{\partial C_c}{\partial \zeta}|_w \tag{60}$$

The nondimensional quantities appearing in the above equations are the Reynolds, Prandtl and Lewis numbers defined as:

$$Re \equiv \frac{\overline{\rho}_\infty \overline{U}_\infty \overline{L}_{ref}}{\overline{\mu}_{ref}}$$

$$Pr \equiv \frac{\overline{\mu}\overline{c}_p}{\overline{\kappa}_h}$$

$$Pr_v \equiv \frac{\overline{\mu}\overline{c}_{pv}}{\overline{\kappa}_v}$$

$$Le_s \equiv \frac{\overline{\rho}\overline{D}_s\overline{c}_p}{\overline{\kappa}_h}$$

$$Le_{v,s} \equiv \frac{\overline{\rho}\overline{D}_s\overline{c}_{pv}}{\overline{\kappa}_v}$$

where $\overline{c}_p$ and $\overline{c}_{pv}$ are the frozen specific heat of the mixture and the specific heat of the mixture for vibrationally excited molecules, respectively.

In the governing equations (46)-(52), the specific second-order terms are underlined. These terms become negligible when the radius of curvature is very large compared with the local boundary-layer thickness (first-order theory). Other second-order effects are present in the momentum and energy equations through metric tensor components g_{ij}, which are influenced by the

surface curvature and in turn affect the Christoffel symbols, and the contravariant velocity components U, V, W, which are related to the general base vectors $\underline{g_i}$. It must be noted that a surface-normal momentum equation (49) contains a non-zero pressure gradient term, which results from centrifugal force induced by the surface curvature. The pressure is thus not constant across the boundary layer. In the first-order approximation, the metrics can be estimated on the body surface since there is no significant variation across the boundary layer [19]. Thus, $g_{ij} = a_{\alpha\beta}, (i, j, \alpha, \beta = 1, 2)$, and the number of operations required for a numerical calculation will be significantly reduced.

It is worthy to compare the three-dimensional second-order boundary-layer equations (46)-(52) with the three-dimensional viscous-shock-layer equations [41-44] in a non-orthogonal, surface-oriented coordinate system. In the viscous-shock-layer analysis of Ref. 41-44, all terms up to second order in ε, where $\varepsilon = Re^{-\frac{1}{2}}$ is the Reynolds number parameter, are retained in the normalized steady Navier-Stokes equations. Also, all viscous terms in the normal momentum equation are neglected to eliminate the cross derivatives that appear. The resulting viscous-shock-layer (VSL) equations are the same to the second-order boundary-layer equations (46)-(52) except for the surface normal momentum equation (49). By additionally applying thin layer approximation to the normal momentum equation, the hyperbolic-parabolic nature of the VSL equations can be changed to the totally parabolic nature of the second-order boundary-layer equations [45].

The perfect gas boundary-layer equations can be easily obtained by dropping vibrational-electronic-electron energy equation (50) and species continuity equation (52) and modifying overall energy equation (51). The resulting equations are identical with the system of equations previously developed by Panaras [23].

As explained in 2.1.1, once the geometrical structure of the body surface is defined, one can calculate the metric tensor and the Christoffel symbols. These geometric quantities are then substituted into the boundary-layer equations (46)-(52).

2.4 Boundary Conditions

The boundary conditions at the wall are prescribed by the usual non-slip conditions. The velocities at the wall are given by

$$U(\xi,\eta,\zeta=0)=V(\xi,\eta,\zeta=0)=W(\xi,\eta,\zeta=0)=0 \tag{61}$$

The translational-rotational temperature at the wall may be given by either the prescribed wall temperature or the prescribed heat flux through the surface. That is:

$$T(\xi,\eta,\zeta=0)=T_w(\xi,\eta) \tag{62}$$

or

$$\frac{\partial T(\xi,\eta,\zeta=0)}{\partial\zeta}=\frac{\partial T_w(\xi,\eta)}{\partial\zeta} \tag{63}$$

The $T_e=T_v$ approximation may not be valid in the boundary layer adjacent to the wall, where electrons are affected by the electrical field produced by a charge separation (the plasma-sheath effects) [46]. Consequently, the electron temperature T_e and the electron pressure p_e at the wall must be derived using the plasma-sheath theory discussed in Ref. 46. However, we tentatively ignore the plasma-sheath effects for simplicity and assume $T_e=T_v$ at the wall. Then the vibrational-electronic-electron temperature T_v at the wall is given by

$$T_v(\xi,\eta,\zeta=0)=T_w(\xi,\eta) \tag{64}$$

or

$$\frac{\partial T_v(\xi,\eta,\zeta=0)}{\partial\zeta}=\frac{\partial T_w(\xi,\eta)}{\partial\zeta} \tag{65}$$

The body is assumed to have a fully catalytic or noncatalytic wall. Then, the species concentration at the wall can be expressed by

$$C_s(\xi,\eta,\zeta=0)=C_{sw}(\xi,\eta);\quad (for\ fully\ catalytic\ wall) \tag{66}$$

or

$$\frac{\partial C_s(\xi,\eta,\zeta=0)}{\partial\zeta}=0;\quad (for\ noncatalytic\ wall) \tag{67}$$

Usually, $C_{sw}(\xi,\eta)$ are not known a priori and therefore must be determined from the species mass flux balance at the wall. However, for simplicity, $C_{sw}(\xi,\eta)$ are chosen here to be equilibrium values with a specified temperature and a pressure. For more general catalytic boundary conditions for the species conservation equations, see Ref. 32.

The outer boundary conditions are derived from the matching between the viscous and the inviscid profiles at the boundary-layer outer edge. In first-order theory, this leads to the assumption that the inviscid flow across the boundary layer is constant and equal to its value at the wall.

$$\begin{aligned} U(\xi,\eta,\zeta=\delta) &= U_{ed}(\xi,\eta,\zeta=\delta) \\ &= U_{ed}(\xi,\eta,\zeta=0) \end{aligned} \tag{68}$$

$$\begin{aligned} V(\xi,\eta,\zeta=\delta) &= V_{ed}(\xi,\eta,\zeta=\delta) \\ &= V_{ed}(\xi,\eta,\zeta=0) \end{aligned} \tag{69}$$

In second-order theory, the matching between the boundary layer and the external inviscid flow must be fitted up to the second order. Monnoyer [15, 16] deduced the following equivalent inviscid velocity distribution across the boundary layer assuming that the outer inviscid flow is irrotational:

$$U(\xi,\eta,\zeta=\delta) = g^{11}a_{11}U_{ed}(\xi,\eta,\zeta=0) \tag{70}$$

$$V(\xi,\eta,\zeta=\delta) = g^{22}a_{22}V_{ed}(\xi,\eta,\zeta=0) \tag{71}$$

The relations (70) and(71) reflect the skewing of the inviscid velocity flow field across the boundary layer. That is, the velocity vector $\underline{v}_{ed}$ is not contained in one plane normal to the surface as in the first-order theory. Instead, the angle between the x^1 line at the wall and $\underline{v}_{ed}$ varies across the boundary layer. The rationale of these arguments can be found in Ref. 15. All other flow variables at the outer edge such as temperature, pressure and species concentrations are interpolated from the inviscid solution profiles.

2.5 Displacement Thickness

The displacement thickness δ_1 is an important boundary-layer parameter in the evaluation of the extent of the viscous flow field. Assuming that the boundary-layer thickness δ, as well as the velocity distribution along the normal to the wall are known at any point on the body surface (strictly speaking, the boundary-layer thickness must be determined in the solution process by a condition of smooth merging of boundary-layer flow into the

outer inviscid flow), the displacement thickness δ_1 is defined in such a way that the mass flux in the presence of the boundary layer is the same as the mass flux in a inviscid flow terminating at δ_1 instead of the wall [15, 16]. This definition leads to the relationship:

$$\frac{\partial}{\partial\xi}(\sqrt{a}\int_0^{\delta} M[\rho_{ed}U_{ed} - \rho U]d\zeta) = \frac{\partial}{\partial\xi}(\sqrt{a}\int_0^{\delta_1} M\rho_{ed}U_{ed}d\zeta) \tag{72}$$

$$\frac{\partial}{\partial\eta}(\sqrt{a}\int_0^{\delta} M[\rho_{ed}V_{ed} - \rho V]d\zeta) = \frac{\partial}{\partial\eta}(\sqrt{a}\int_0^{\delta_1} M\rho_{ed}V_{ed}d\zeta) \tag{73}$$

where $a = det(\alpha_{\alpha\beta}) = a_{11}a_{22} - (a_{12})^2$.
M is given by [19]

$$M = 1 - (K_1 + K_2)\zeta + K_1K_2\zeta^2 \tag{74}$$

where K_1 and K_2 are the principal curvatures of the surface. Equations (72) and (73) are integro-differential equations for the unknown displacement thickness δ_1 which must be solved iteratively after all the flow variables are known. The displacement effect of the boundary layer on the external inviscid flow can be dealt with by means of an effective thickening of the body, which requires the body geometry to be readjusted during the viscous-inviscid matching process.

An alternative way of imposing the displacement effect is the equivalent source distribution proposed by Lighthill [47]. For the surface $\zeta = \delta_1(\xi, \eta)$ to be an inviscid streamline surface, an equivalent wall outflow $(\rho_e W_e)_w$ has to be applied which obeys the relationship [15, 16] :

$$\sqrt{a}(\rho_{ed}W_{ed})_w = \frac{\partial}{\partial\xi}(\sqrt{a}\int_0^{\delta_1} M\rho_{ed}U_{ed}d\zeta) \tag{75}$$

$$\sqrt{a}(\rho_{ed}W_{ed})_w = \frac{\partial}{\partial\eta}(\sqrt{a}\int_0^{\delta_1} M\rho_{ed}V_{ed}d\zeta) \tag{76}$$

Combining equations (72), (73), (75) and (76) provides the following relationship which no longer includes δ_1:

$$(\rho_{ed}W_{ed})_w = \frac{1}{2\sqrt{a}}\{\frac{\partial}{\partial\xi}(\sqrt{a}\int_0^{\delta} M[\rho_{ed}U_{ed} - \rho U]d\zeta) + \frac{\partial}{\partial\eta}(\sqrt{a}\int_0^{\delta} M[\rho_{ed}V_{ed} - \rho V]d\zeta)\} \tag{77}$$

The equivalent source distribution can be calculated from equation (77) once the boundary layer solution is obtained. The influence of the boundary layer on the inviscid flow is then accounted for by a distribution of equivalent source distribution at the wall (77).

A matching of the boundary-layer flow to the external inviscid flow can be achieved by an iterative process in which the outer flow is modified by the newly computed displacement effect. The resulting equivalent inviscid flow is then further coupled with the boundary layer by providing the new boundary conditions at the boundary-layer outer edge. In addition, the other second-order effects such as the entropy and total enthalpy gradient effects, which originate in the inviscid part of the flow, can be taken into account in the calculation by matching process. Consequently, in the future paper it is necessary to address the numerical methods for the boundary-layer solution, the computational algorithms for the inviscid Euler solution, and the viscous-invicid techniques.

2.6 Thermodynamic and Transport Properties

In the calculation of viscous flow over hypersonic vehicles, the correct evaluation of the heat transfer rate to the body surface is strongly subject to the accuracy of the thermodynamic and transport properties which involve uncertainties in the high temperature regime especially in the thermal nonequilibrium multi-temperature environments. The nonequilibrium flow environments surrounding these vehicles will significantly impact the aerodynamic and thermal loads to the vehicles. Consequently, aerothermodynamic evaluation under these circumstances requires a reasonable model for these physical properties. Lee [29] developed an explicit formula for the nonequilibrium thermodynamic and transport properties based on the three-temperature concept (translational-rotational, vibrational, and electron-electronic excitation temperatures). To derive the nonequilibrium thermodynamic properties, it is assumed that 1) the rotational mode of molecules is fully equilibrated with the translational mode of heavy particles and that 2) the population densities of vibrational and electronic excitation energy levels have Boltzmann distributions with a vibrational temperature $\overline{T}_v$ and an electron temperature $\overline{T}_e$. In addition, an assumption is made that there is no coupling of energy level between these modes. The nonequilibrium transport prop-

erties are evaluated by assuming that all distribution functions are close to Maxwellian about their inherent temperature, that is, $\overline{T}$ for heavy particles (molecules, atoms, and ions) and $\overline{T}_e$ for electrons.

2.6.1 Thermodynamic Properties

By slightly modifying the formulation of Lee [29], the vibrational energy of the mixture $\overline{e}_v$ can be expressed by

$$\overline{e}_v = \frac{\sum_{s=1}^{11} \overline{\rho}_s \overline{e}_{v,s}}{\overline{\rho}} \tag{78}$$

where $\overline{e}_{v,s}$ is the vibrational energy for species s given by

$$\overline{e}_{v,s} = \int_{\overline{T}_{ref}}^{\overline{T}_v} \overline{c}_{vv,s} d\overline{T}' \tag{79}$$

where $\overline{c}_{vv,s}$ is the specific heat of species s at constant volume for vibrational excitation, and $\overline{T}'$ is the dummy variable of integration. It must be noted that $\overline{e}_{v,s}$ is zero for atoms and electrons ($s = 1, 2, 6, 7, 11$).

The electronic energy of mixture $\overline{e}_{el}$ is given by

$$\overline{e}_{el} = \frac{\sum_{s=1}^{11} \overline{\rho}_s \overline{e}_{el,s}}{\overline{\rho}} \tag{80}$$

where $\overline{e}_{el,s}$ is defined as the electronic excitation energy for species s except for electrons. For species s, $\overline{e}_{el,s}$ is expressed by

$$\overline{e}_{el,s} = \int_{\overline{T}_{ref}}^{\overline{T}_e} \overline{c}_{vel,s} d\overline{T}' = \int_{\overline{T}_{ref}}^{\overline{T}_v} \overline{c}_{vel,s} d\overline{T}' \tag{81}$$

where $\overline{c}_{vel,s}$ is the specific heat of species s at constant volume for electronic excitation.

For electrons, $\overline{e}_{el,e}$ is defined as the translational energy of electrons, i.e.,

$$\overline{e}_{el,e} = \overline{e}_e = \frac{3}{2}\left(\frac{\overline{\Re}}{\overline{M}_e}\right)\overline{T}_e = \frac{3}{2}\left(\frac{\overline{\Re}}{\overline{M}_e}\right)\overline{T}_v \tag{82}$$

The vibrational enthalpy of species s, $\overline{h}_{v,s}$, is identical to the vibrational energy $\overline{e}_{v,s}$ for molecular species s.
The electronic enthalpy of species s, $\overline{h}_{el,s}$, becomes identical to $\overline{e}_{el,s}$ for all species except electrons. For electrons, $\overline{h}_{el,e}$ is given by

$$\overline{h}_{el,e} = \overline{e}_{el,e} + (\frac{\overline{\Re}}{\overline{M}_e})\overline{T}_e = \frac{5}{2}(\frac{\overline{\Re}}{\overline{M}_e})\overline{T}_v \tag{83}$$

The enthalpy for species s, $\overline{h}_s$, for the present two-temperature model is given by

$$\overline{h}_s = \int_{\overline{T}_{ref}}^{\overline{T}} (\overline{c}_{pt,s} + \overline{c}_{pr,s})d\overline{T}' + \int_{\overline{T}_{ref}}^{\overline{T}_v} \overline{c}_{pv,s}d\overline{T}' + \int_{\overline{T}_{ref}}^{\overline{T}_e} \overline{c}_{pel,s}d\overline{T}' + \overline{h}_s^0 \tag{84}$$

$\overline{c}_{pt,s}$, $\overline{c}_{pr,s}$, $\overline{c}_{pv,s}$ and $\overline{c}_{pel,s}$ are the specific heats at constant pressure for species s for translation, rotational excitation, vibrational excitation and electronic excitation respectively, and $\overline{h}_s^0$ is the heat of formation.
The frozen specific heat of the mixture $\overline{c}_p$, the specific heat of the mixture for vibrationally excited molecules $\overline{c}_{pv}$ and the specific heat of the mixture for electronic excitation $\overline{c}_{pel}$ are defined by

$$\overline{c}_p = \sum_{s=1}^{11} C_s(\overline{c}_{pt,s} + \overline{c}_{pr,s}) \tag{85}$$

$$\overline{c}_{pv} = \sum_{s=1}^{11} C_s\overline{c}_{pv,s} \tag{86}$$

$$\overline{c}_{pel} = \sum_{s=1}^{11} C_s\overline{c}_{pel,s} \tag{87}$$

Since both the translational and rotational modes are assumed to be fully excited, the specific heats for those modes therefore reduce to [29]

$$\overline{c}_{vt,s} = \frac{3}{2}\frac{\overline{\Re}}{\overline{M}_s} \tag{88}$$

for the translational mode of species s including electrons, and

$$\overline{c}_{vr,s} = \frac{\overline{\Re}}{\overline{M}_s} \tag{89}$$

for the rotational mode.

The internal modes separation assumption is valid only at low temperatures. At sufficiently high temperatures, the coupling effects between rotation-vibration modes and rotation-vibration-electronic modes become important when evaluating the internal partition functions from which the corresponding specific heats can be derived. Balakrishnan [48] evaluated the partition functions for internal modes by introducing correction factors and generated the following curve fit formula for the vibrational and electronic specific heats:

$$\overline{c}_{vv,s} = \left(\frac{4.186 \cdot 10^7}{\overline{M}_s}\right)\left(\overline{A}_{v,s} + \overline{B}_{v,s}\overline{T}_v + \frac{\overline{C}_{v,s}}{\overline{T}_v^2}\right) \tag{90}$$

$$\overline{c}_{vel,s} = \left(\frac{4.186 \cdot 10^7}{\overline{M}_s}\right)\left(\overline{A}_{el,s} + \overline{B}_{el,s}\overline{T}_e + \frac{\overline{C}_{el,s}}{\overline{T}_e^2}\right) \tag{91}$$

where $\overline{A}$, $\overline{B}$, and $\overline{C}$ are constants in the above polynomial equations and are presented in Ref. 48.

For the translational mode, the following thermodynamic relation applies [29]:

$$\overline{c}_{pt,s} = \overline{c}_{vt,s} + \frac{\overline{\mathfrak{R}}}{\overline{M}_s} \tag{92}$$

For internal modes,

$$\overline{c}_{pz,s} = \overline{c}_{vz,s} \tag{93}$$

where z represents r, v, or el.

2.6.2 Transport Properties

In Ref. 29, the transport properties are evaluated by extending Yos's formula [49], which is based on the first Chapman-Enskog approximation, to the three-temperature gas mixture. In Lee's analysis [29], the controlling temperature in the collision integrals is assumed to be the electron temperature $\overline{T}_e$ for collisions involving electrons, and the heavy-particle translational temperature $\overline{T}$ otherwise. By setting $\overline{T}_e = \overline{T}_v$, the necessary transport properties can be obtained for the present two-temperature approximation.

In the subsequent evaluations of transport properties, two modified collision integrals, $\overline{\Delta}_{sr}^{(1)}(\overline{T})$ and $\overline{\Delta}_{sr}^{(2)}(\overline{T})$, and the molar concentration of species s, $\overline{\gamma}_s$, are extensively used. These quantities are defined by

$$\overline{\Delta}_{sr}^{(1)}(\overline{T}) = \frac{8}{3}\left[\frac{2\overline{M}_s\overline{M}_r}{\pi\overline{\Re}\overline{T}(\overline{M}_s+\overline{M}_r)}\right]^{1/2}\pi\overline{\Omega}_{sr}^{(1,1)} \tag{94}$$

$$\overline{\Delta}_{sr}^{(2)}(\overline{T}) = \frac{16}{5}\left[\frac{2\overline{M}_s\overline{M}_r}{\pi\overline{\Re}\overline{T}(\overline{M}_s+\overline{M}_r)}\right]^{1/2}\pi\overline{\Omega}_{sr}^{(2,2)} \tag{95}$$

$$\overline{\gamma}_s = \frac{\overline{\rho}_s}{\overline{\rho}\overline{M}_s} = \frac{C_s}{\overline{M}_s} \tag{96}$$

The collision integrals $\pi\overline{\Omega}_{sr}^{(1,1)}$ and $\pi\overline{\Omega}_{sr}^{(2,2)}$ for an 11-species air model are evaluated and curve-fitted as a function of temperature in Ref. 50, and tabular version of the data are presented in Ref. 40.

The viscosity of the mixture $\overline{\mu}$ is given by

$$\overline{\mu} = \sum_{s=1}^{10}\frac{\overline{m}_s\overline{\gamma}_s}{\sum_{r=1}^{10}\overline{\gamma}_r\overline{\Delta}_{sr}^{(2)}(\overline{T}) + \overline{\gamma}_e\overline{\Delta}_{se}^{(2)}(\overline{T}_v)} + \frac{\overline{m}_e\overline{\gamma}_e}{\sum_{r=1}^{11}\overline{\gamma}_r\overline{\Delta}_{er}^{(2)}(\overline{T}_v)} \tag{97}$$

The translational thermal conductivity κ_t of heavy particles is expressed as

$$\overline{\kappa}_t = \frac{15}{4}\overline{k}\sum_{s=1}^{10}\frac{\overline{\gamma}_s}{\sum_{r=1}^{10}a_{sr}\overline{\gamma}_r\overline{\Delta}_{sr}^{(2)}(\overline{T}) + 3.54\overline{\gamma}_e\overline{\Delta}_{se}^{(2)}(\overline{T}_v)} \tag{98}$$

where a_{sr} is defined by

$$a_{sr} = 1 + \frac{[1-(m_s/m_r)][0.45-2.54(m_s/m_r)]}{[1+(m_s/m_r)]^2} \tag{99}$$

The rotational thermal conductivity of mixture $\overline{\kappa}_r$ is expressed as

$$\overline{\kappa}_r = \overline{k}\sum_{s=M}\frac{\overline{\gamma}_s}{\sum_{r=1}^{10}\overline{\gamma}_r\overline{\Delta}_{sr}^{(1)}(\overline{T}) + \overline{\gamma}_e\overline{\Delta}_{se}^{(1)}(\overline{T}_v)} \tag{100}$$

Thus, the frozen thermal conductivity of the mixture $\overline{\kappa}_h$ for translational-rotational energy of heavy particles is given by

$$\overline{\kappa}_h = \overline{\kappa}_t + \overline{\kappa}_r \tag{101}$$

The vibrational thermal conductivity of the mixture $\overline{\kappa}_v$ is equal to the rotational thermal conductivity $\overline{\kappa}_r$. That is,

$$\overline{\kappa}_v = \overline{\kappa}_r \tag{102}$$

The V-V thermal conductivity $\overline{\kappa}'_v$ in Eq. (49), which originates exclusively in molecule-molecule collisions, can be written as

$$\overline{\kappa}'_v = \overline{\kappa}_v \sum_{s=M} \frac{\sum_{r=M} \overline{\gamma}_r \overline{\Delta}^{(2)}_{sr}(\overline{T})}{\sum_{r=1}^{10} \overline{\gamma}_r \overline{\Delta}^{(2)}_{sr}(\overline{T}) + \overline{\gamma}_e \overline{\Delta}^{(2)}_{se}(\overline{T}_v)} \tag{103}$$

The electron thermal conductivity $\overline{\kappa}_e$ is given by

$$\overline{\kappa}_e = \frac{15}{4}\overline{k} \frac{\overline{\gamma}_e}{\sum_{r=1}^{11} 1.45 \overline{\gamma}_r \overline{\Delta}^{(2)}_{er}(\overline{T}_v)} \tag{104}$$

The thermal conductivity of electrons $\overline{\kappa}'_e$ due to collisions only between electrons is given by

$$\overline{\kappa}'_e = \overline{\kappa}_e \frac{\overline{\gamma}_e \overline{\Delta}^2_{ee}(\overline{T}_v)}{\sum_{r=1}^{11} \overline{\gamma}_r \overline{\Delta}^2_{er}(\overline{T}_v)} \tag{105}$$

The binary diffusion coefficient of an $s-r$ pair of heavy particles is given by

$$\overline{D}_{sr} = \frac{\overline{kT}}{\overline{p}\overline{\Delta}^{(1)}_{sr}(\overline{T})} \tag{106}$$

where $\overline{p}$ is the pressure.

The binary diffusion coefficient between electrons and heavy particles is expressed as

$$\overline{D}_{er} = \frac{\overline{kT}_v}{\overline{p}\overline{\Delta}^{(1)}_{er}(\overline{T}_v)} \tag{107}$$

The effective diffusion coefficient of species s is then defined as

$$\overline{D}_s = \frac{\overline{\gamma}_t^2 \overline{M}_s (1 - \overline{M}_s \overline{\gamma}_s)}{\sum_{r=1 r \neq s}^{11} (\overline{\gamma}_r / \overline{D}_{sr})} \tag{108}$$

where the total molar concentration of the mixture $\overline{\gamma}_t$ is defined by

$$\overline{\gamma}_t = \sum_{s=1}^{11} \overline{\gamma}_s \tag{109}$$

For ions, the ambipolar diffusion coefficient $\overline{D}_s^a$, which has the double value of the ionic diffusion coefficient $\overline{D}_s$, is introduced due to the ambipolar diffusion approximation [29]; that is

$$\overline{D}_s^a = 2\overline{D}_s \quad (s = 6,7,8,9,10) \tag{110}$$

Then, the effective diffusion coefficient of electrons $\overline{D}_e$ is expressed by

$$\overline{D}_e = \overline{m}_e \frac{\sum_{s=6}^{10} \overline{D}_s^a \overline{\gamma}_s}{\sum_{s=6}^{10} \overline{m}_s \overline{\gamma}_s} \tag{111}$$

2.7 Chemical Kinetic Model

Under chemical and thermal nonequilibrium environments, there are coupling phenomena among the internal energy modes and between chemical processes and the internal modes. Therefore, the chemical reaction rate coefficients are no longer a function of a single temperature. Furthermore, several energy reactive source terms and physical properties originated in the energy exchange processes appear in the vibrational-electronic-electron energy equation (34) or (50).

2.7.1 Chemical Reaction Rate Coefficients

Park [36, 37] proposed a controlling-temperature concept for certain types of reactions and assessed its validity by comparing the calculated results with the available experimental data for nitrogen and air. He suggested using a geometrical average temperature $\overline{T}_a$ as a controlling temperature for dissociative reactions which implicitly accounts for the vibration-dissociation coupling. The average temperature $\overline{T}_a$ is defined by

$$\overline{T}_a = \overline{T}^q \overline{T}_v^{(1-q)} \quad (q = 0.5 \text{ or } 0.7) \tag{112}$$

He also suggests that the controlling temperature for the electron impact ionization is $\overline{T}_e$ ($\overline{T}_v$ for a two-temperature model). All other reactions are characterized by the translational-rotational temperature $\overline{T}$. Park recommended the rate coefficients for the chemical reactions in the nonequilibrium

high temperature air be expressed as a function of the controlling temperature, and tabulated forward reaction rate coefficients $\overline{k}_{f,p}$ for 11 air species with 33 reactions [51]. The backward reaction rate coefficient $\overline{k}_{b,p}$ is related to the forward reaction rate coefficient through the equilibrium constant $\overline{K}_{c,p}$ in the form

$$\overline{k}_{b,p} = \frac{\overline{k}_{f,p}}{\overline{K}_{c,p}} \tag{113}$$

Park [52] generated the empirical formula for the equilibrium constant $\overline{K}_{c,p}$ with polynomial functions of translational-rotational temperature $\overline{T}$.

2.7.2 Reactive Source Terms

The effective collision frequency of electrons $\overline{\nu}^*_{er}$, which appears in the elastic energy exchange term between electrons and heavy particles in Eq. (34) or (50), is explained in detail in Ref. 29.

The vibrational energy reactive source term $\overline{\dot{w}}_s \overline{D}^v_s$ represents the rate of change of vibrational energy of the diatomic molecules due to dissociation or recombination. The electronic energy reactive source term $\overline{\dot{n}}_{e,s} \overline{E}_{i,s}$ accounts for the rate of electron energy loss due to electron-impact ionization. These two terms are discussed in Ref. 40 and the tabulated values are presented there.

2.8 Vibrational Relaxation

The rate of change in the population of the vibrational states at low temperatures is described well by an equation of the Landau-Teller form [54]. However, at high vibrational temperatures the vibrational energy exchange process is primarily governed by a comparatively slow diffusion process [38]. A bridging function between the faster Landau-Teller relaxation rate and the slower diffusive rate has been proposed by Park [36, 37, 53]. The resulting expression for the translation-vibration (T-V) energy exchange term in Eq. (34) or (50) is

$$\overline{\rho} C_s \frac{\overline{e}^*_{v,s} - \overline{e}_{v,s}}{\overline{\tau}_s} \left| \frac{\overline{T}_{sh} - \overline{T}_v}{\overline{T}_{sh} - \overline{T}_{v,sh}} \right|^{s_s}$$

where the bridging function, S_s, is given by

$$S_s = 3.5exp(-\overline{\theta}_s/\overline{T}_{sh}) \tag{114}$$

The quantities $\overline{T}_{sh}$ and $\overline{T}_{v,sh}$ are the translational-rotational and vibrational temperatures immediately behind the bow shock wave. The characteristic temperature, $\overline{\theta}_s$, for molecular species s are listed in Ref. 55.

The relaxation time of species s, $\overline{\tau}_s$ is given as a combination of the Landau-Teller type relaxation time and the collision limited relaxation time such that

$$\overline{\tau}_s = < \overline{\tau}_s > + \overline{\tau}_{cs} \tag{115}$$

The average relaxation time $< \overline{\tau}_s >$ is defined as [29]

$$< \overline{\tau}_s >= \frac{\sum_{r=1}^{10} \overline{\gamma}_r}{\sum_{r=1}^{10} \frac{\overline{\gamma}_r}{\overline{\tau}_{sr}}} \tag{116}$$

where $\overline{\tau}_{sr}$ is the T-V relaxation time for molecular species s with collision partner r, and is usually determined by the semiempirical correlations of Millikan and White [54]. The collision limited relaxation time $\overline{\tau}_{cs}$ is given by [36, 37]

$$\overline{\tau}_{cs} = \frac{1}{\overline{c}_s \overline{\sigma}_v \overline{N}_s} \tag{117}$$

$\overline{N}_s$ is the number density of species s, and $\overline{c}_s$ is the average molecular speed of species s, expressed by

$$\overline{c}_s = (8\overline{\Re T}/\pi \overline{M}_s)^{1/2} \tag{118}$$

The expression for the limiting collision cross section, $\overline{\sigma}_v$, is assumed to be [53]

$$\overline{\sigma}_v = 10^{-21}(50,000/\overline{T})^2 \ \ m^2 \tag{119}$$

3. Stagnation-Point Flow

3.1 Basic Equations for Stagnation Flow

If the origin of the coordinate system is at the stagnation point, then the boundary-layer equations can be solved by marching away from the stagnation point. One must first determine the stagnation point location and then needed grid. This can be done by solving the Euler equations in the Cartesian coordinate system. The stagnation point location is determined by interpretating the inviscid flow properties between Cartesian grid points. The origin of the coordinates for the Euler equations then is shifted to the obtained stagnation point location. At the same time, the boundary-layer coordinate system originates from the stagnation point is considered [56]. This technique has been successfully used in the axisymmetric analog method [3, 4, 57, 58] to compute approximately the three-dimensional boundary layers. In this approach, the surface streamlines which start from the stagnation point are calculated by using either surface velocity or pressure obtained from the inviscid flow solution. To ensure the efficiency and accuracy in the viscous-inviscid coupling, it is desirable to choose the new Euler grid after the origin shfting coincides with the boundary-layer grid on the body surface. Thus, interpolation between the Euler and the boundary-layer grid points becomes necessary in surface normal direction only.

In order to start the boundary-layer solution from the three-dimensional stagnation point, it is necessary to obtain the stagnation-point equations and their solutions first. We let the origin of the surface-oriented coordinate system (ξ, η, ζ) coincide with the stagnation point S on the body surface. That is

$$S = S(\xi = \eta = \zeta = 0) \tag{120}$$

It is assumed that the stagnation line is a straight line normal to the body surface. In accordance with the approach of Hirschel and Kordulla [19], we assume further that the body surface is not too strongly curved in the vicinity of the stagnation point, and that the body and the flow past it, and therefore the flow variables, are symmetric in regard to two planes ($\xi = 0$ and $\eta = 0$) at the stagnation point.

$$\xi = 0, \quad \eta = 0, \quad \zeta \geq 0 :$$

$$\frac{\partial U^*}{\partial \eta} = \frac{\partial V^*}{\partial \xi} = 0$$
$$\frac{\partial T}{\partial \xi} = \frac{\partial T}{\partial \eta} = \frac{\partial T_v}{\partial \xi} = \frac{\partial T_v}{\partial \eta} = \frac{\partial h}{\partial \xi} = \frac{\partial h}{\partial \eta} = \frac{\partial e_V}{\partial \xi} = \frac{\partial e_V}{\partial \eta} = 0$$
$$\frac{\partial \rho}{\partial \xi} = \frac{\partial \rho}{\partial \eta} = \frac{\partial p}{\partial \xi} = \frac{\partial p}{\partial \eta} = \frac{\partial p_e}{\partial \xi} = \frac{\partial p_e}{\partial \eta} = \frac{\partial C_s}{\partial \xi} = \frac{\partial C_s}{\partial \eta} = 0 \qquad (121)$$

The definition of a three-dimensional stagnation point is given by [19]

$$\xi = 0, \ \eta = 0, \ \zeta \geq 0 :$$
$$U^* = V^* = 0$$
$$\frac{\partial U^*}{\partial \xi} \neq 0, \ \frac{\partial V^*}{\partial \eta} \neq 0 \qquad (122)$$

Here, new dependent variables at the stagnation line ($\xi = 0, \eta = 0, \zeta \geq 0$) are introduced

$$A^1(\zeta) \equiv \frac{\partial U}{\partial \xi} \qquad A^2(\zeta) \equiv \frac{\partial V}{\partial \eta} \qquad (123)$$

Since the variables W, A^1, A^2, ρ, p, p_e, T, T_v and C_s are functions of only ζ along the stagnation line by definition, the following set of ordinary differential equations can be obtained by applying the conditions (121) and (122) to the boundary-layer equations (46)-(52):

Continuity:

$$\rho(A^1 + A^2) + \frac{1}{\sqrt{g}} \frac{d(\rho W \sqrt{g})}{d\zeta} = 0 \qquad (124)$$

ξ-momentum:

$$\rho(A^1)^2 + \rho W \frac{dA^1}{d\zeta} = \rho_{ed}(A^1_{ed})^2 + \frac{1}{Re} \frac{d}{d\zeta}(\mu \frac{dA^1}{d\zeta}) + \underline{\frac{1}{Re} \frac{1}{\sqrt{g}} \mu \frac{dA^1}{d\zeta} \frac{d\sqrt{g}}{d\zeta}} + \underline{\frac{2\mu}{Re} \Gamma^1_{31} \frac{dA^1}{d\zeta}} \qquad (125)$$

η-momentum:

$$\rho(A^2)^2 + \rho W \frac{dA^2}{d\zeta} = \rho_{ed}(A^2_{ed})^2 + \frac{1}{Re} \frac{d}{d\zeta}(\mu \frac{dA^2}{d\zeta}) + \underline{\frac{1}{Re} \frac{1}{\sqrt{g}} \mu \frac{dA^2}{d\zeta} \frac{d\sqrt{g}}{d\zeta}} + \underline{\frac{2\mu}{Re} \Gamma^2_{23} \frac{dA^2}{d\zeta}} \qquad (126)$$

ζ-momentum:

$$\frac{dp}{d\zeta} = 0 \tag{127}$$

Vibrational-electronic-electron energy:

$$\begin{aligned}\rho W\frac{de_V}{d\zeta} &= p_e\frac{dW}{d\zeta} + \frac{1}{Re}\frac{d}{d\zeta}[(\kappa_v' + \kappa_e)\frac{dT_v}{d\zeta}] + \underline{\frac{1}{Re}\frac{d}{d\zeta}\frac{(\kappa_v' + \kappa_e)}{\sqrt{g}}\frac{d\sqrt{g}}{d\zeta}\frac{dT_v}{d\zeta}} \\ &+ \frac{1}{Re}\frac{d}{d\zeta}(\sum_{s=1}^{11}\frac{\mu Le_{v,s}}{Pr_v}h_{V,s}\frac{dC_s}{d\zeta}) + \underline{\frac{1}{Re}\frac{1}{\sqrt{g}}\sum_{s=1}^{11}(\frac{\mu Le_{v,s}}{Pr_v}h_{V,s})\frac{d\sqrt{g}}{d\zeta}\frac{dC_s}{d\zeta}} \\ &+ \rho\sum_{s=M}C_s\frac{e^*_{v,s} - e_{v,s}}{\tau_s}|\frac{T_{sh} - T_v}{T_{sh} - T_{v,sh}}|^{S_s-1} + 3(\frac{\overline{R}}{\overline{c}_{p\infty}})\rho(T - T_v)\sum_{s=1}^{10}\frac{\mu^*_{cr}}{M_r} \\ &- \sum_{s=6}^{10}\dot{n}_{e,s}E_{i,s} + \sum_{s=M}\dot{w}_sD_s^v \end{aligned} \tag{128}$$

Overall energy:

$$\begin{aligned}\rho W\frac{dh}{d\zeta} &= \frac{1}{Re}\frac{d}{d\zeta}(\kappa_h\frac{dT}{d\zeta}) + \underline{\frac{1}{Re}\frac{\kappa_h}{\sqrt{g}}\frac{d\sqrt{g}}{d\zeta}\frac{dT}{d\zeta}} \\ &+ \frac{1}{Re}\frac{\partial}{\partial\zeta}[(\kappa_v + \kappa_e)\frac{\partial T_v}{\partial\zeta}] + \underline{\frac{1}{Re}\frac{(\kappa_v + \kappa_e)}{\sqrt{g}}\frac{\partial\sqrt{g}}{\partial\zeta}\frac{\partial T_v}{\partial\zeta}} \\ &+ \frac{1}{Re}\frac{d}{d\zeta}(\sum_{s=1}^{11}\frac{\mu Le_s}{Pr}h_s\frac{dC_s}{d\zeta}) + \underline{\frac{1}{Re}\frac{1}{\sqrt{g}}\sum_{s=1}^{11}(\frac{\mu Le_s}{Pr}h_s)\frac{d\sqrt{g}}{d\zeta}\frac{dC_s}{d\zeta}} \end{aligned} \tag{129}$$

Species continuity:

$$\begin{aligned}\rho W\frac{dC_s}{d\zeta} &= \frac{1}{Re}\frac{1}{d\zeta}(\frac{\mu Le_s}{Pr}\frac{dC_s}{d\zeta}) \\ &+ \underline{\frac{1}{Re}\frac{1}{\sqrt{g}}\frac{\mu Le_s}{Pr}\frac{d\sqrt{g}}{d\zeta}\frac{dC_s}{d\zeta}} + \dot{w}_s; \quad (s = 1, 2, \ldots, 11) \end{aligned} \tag{130}$$

The equations (125) and (126) are obtained by differentiating the momentum equations (47) and (48) with respect to ξ and η, respectively. Furthermore,

the pressure gradient terms in the equations (125) and (126) have been replaced by the convective terms at the outer edge of the boundary layer.

$$\rho_{ed}(A^1_{ed})^2 = -\frac{g_{22}}{g}\frac{\partial^2 p}{\partial\xi\partial\xi} + \frac{g_{12}}{g}\frac{\partial^2 p}{\partial\xi\partial\eta} \tag{131}$$

$$\rho_{ed}(A^2_{ed})^2 = \frac{g_{12}}{g}\frac{\partial^2 p}{\partial\xi\partial\eta} - \frac{g_{11}}{g}\frac{\partial^2 p}{\partial\eta\partial\eta} \tag{132}$$

The obtained (6 + NS) equations (124)-(130) plus the equations of state (53) and (54) would determine the (8 + NS) unknown variables W, A^1, A^2, ρ, p, p_e, T, T_v and C_s.

Before solving the equations (124)-(130), a transformation of the normal coordinate may be introduced by changing the independent variable from ζ to χ in such a way that

$$\chi = \frac{\zeta}{\delta} \tag{133}$$

where δ is the local boundary-layer thickness. This transformation, which does not affect the geometrical considerations, gives the effect of fixing the body surface at $\chi = 0$ and the outer boundary-layer edge at $\chi = 1$, and a finite number of grid points can be used over the computational domain $0 \leq \chi \leq 1$.

3.2 Boundary Conditions for Stagnation Flow

The usual boundary conditions at the wall are

$$W(\zeta = 0) = 0 \tag{134}$$

$$A^1(\zeta = 0) = A^2(\zeta = 0) = 0 \tag{135}$$

$$T(\zeta = 0) = T_w \tag{136}$$

or

$$\frac{dT(\zeta = 0)}{d\zeta} = \frac{dT_w}{d\zeta} \tag{137}$$

$$T_v(\zeta = 0) = T_w \tag{138}$$

or

$$\frac{dT_v(\zeta = 0)}{d\zeta} = \frac{dT_w}{d\zeta} \tag{139}$$

$$C_s(\zeta = 0) = C_{sw}; \quad (for\ fully\ catalytic\ wall) \tag{140}$$

or

$$\frac{dC_s(\zeta = o)}{d\zeta} = 0; \quad (for\ noncatalytic\ wall) \tag{141}$$

The velocity W and the partial derivatives of velocities A^1 and A^2 at the outer boundary are

$$W(\zeta = \delta) = W_{ed} \tag{142}$$

$$\begin{aligned} A^1(\zeta = \delta) &= A^1_{ed}(\zeta = \delta) = g^{11}a_{11}A^1_{ed}(\zeta = 0) \\ A^2(\zeta = \delta) &= A^2_{ed}(\zeta = \delta) = g^{22}a_{22}A^2_{ed}(\zeta = 0) \end{aligned} \tag{143}$$

where

$$A^1_{ed}(\zeta) \equiv \frac{\partial U_{ed}}{\partial \xi}, \quad A^2_{ed}(\zeta) \equiv \frac{\partial V_{ed}}{\partial \eta}$$

The outer boundary conditions for pressure, temperatures and species concentration are given by the external inviscid flow solution at the stagnation line.

3.3 Displacement Thickness for Stagnation Flow

By imposing the conditions (121) and (122) into equations (72) and (73), the relation for the displacement thickness along the stagnation line becomes

$$\begin{aligned} &\int_0^{\delta} M[\rho_{ed}(A^1_{ed} + A^2_{ed}) - \rho(A^1 + A^2)]d\zeta \\ &\quad = \int_0^{\delta_1} M\rho_{ed}(A^1_{ed} + A^2_{ed})d\zeta \end{aligned} \tag{144}$$

Similarly, an equivalent wall outflow at the stagnation point is obtained by relation (77)

$$(\rho_{ed} W_{ed})_w = \frac{1}{2} \int_0^\delta M[\rho_{ed}(A^1_{ed} + A^2_{ed}) - \rho(A^1 + A^2)] d\zeta \qquad (145)$$

Since M is defined by equation (74), the equivalent source at the stagnation point can be calculated from equation (145) once the boundary layer solution is obtained.

4. Concluding Remarks

The second-order hypersonic three-dimensional thermochemical nonequilibrium boundary-layer equations in generalized curvilinear coordinates are derived by means of an order-of-magnitude analysis. The two-temperature concept is extensively applied to describe a thermal and chemical nonequilibrium flow around a general body geometry. Corresponding three-dimensional boundary conditions are shown along with the boundary-layer parameters and the invicid-viscous layer matching procedure. In addition, the expressions for the nonequilibrium thermodynamic and transport properties and chemical reaction rates are given. The resulting set of basic equations will be suitable for the development of a boundary-layer computational code which allows simultaneous handling of both general three-dimensional configurations and general thermochemical nonequilibrium gas models in an engineering context. By investigating a systematic analysis of three-dimensional flow and high-temperature nonequilibrium chemico-physics described in the present paper, the future users of the three-dimensional code being developed will be able to have an opportunity to evaluate the accuracy of the governing equations that are being solved numerically (code validation).

Appendix A

Metric Tensors

By applying the definition [equation (7)], the components of the covariant metric tensor in the present partially orthogonal system are given by:

$$\begin{aligned} g_{11} &= x_\xi^2 + y_\xi^2 + z_\xi^2 \quad , \quad g_{12} = g_{21} = x_\xi x_\eta + y_\xi y_\eta + z_\xi z_\eta \\ g_{22} &= x_\eta^2 + y_\eta^2 + z_\eta^2 \quad , \quad g_{13} = g_{31} = g_{23} = g_{32} = 0 \\ g_{33} &= x_\zeta^2 + y_\zeta^2 + z_\zeta^2 = 1 \end{aligned} \qquad (A-1)$$

The components of the contravariant metric tensor can be expressed similarly by the relation (9):

$$\begin{aligned} g^{11} &= \frac{g_{22}}{g} \quad , \quad g^{12} = \frac{-g_{12}}{g} \\ g^{22} &= \frac{g_{11}}{g} \quad , \quad g^{13} = g^{31} = g^{23} = g^{32} = 0 \\ g^{33} &= \frac{g_{11}g_{22} - g_{12}^2}{g} = 1 \end{aligned} \qquad (A-2)$$

Appendix B

Christoffel Symbols

The Christoffel symbols of the second kind are given here for the present semiorthogonal coordinate system:

$$\Gamma^1_{11} = \frac{1}{2g}[g_{22}\frac{\partial g_{11}}{\partial \xi} - g_{12}(2\frac{\partial g_{12}}{\partial \xi} - \frac{\partial g_{11}}{\partial \eta})] \qquad (B-1)$$

$$\Gamma^1_{21} = \Gamma^1_{12} = \frac{1}{2g}[g_{22}\frac{\partial g_{11}}{\partial \eta} - g_{12}\frac{\partial g_{22}}{\partial \xi}] \qquad (B-2)$$

$$\Gamma^1_{22} = \frac{1}{2g}[g_{22}(2\frac{\partial g_{12}}{\partial \eta} - \frac{\partial g_{22}}{\partial \xi}) - g_{12}\frac{\partial g_{22}}{\partial \eta}] \qquad (B-3)$$

$$\Gamma^2_{11} = \frac{1}{2g}[g_{11}(2\frac{\partial g_{12}}{\partial \xi} - \frac{\partial g_{11}}{\partial \eta}) - g_{12}\frac{\partial g_{11}}{\partial \xi}] \qquad (B-4)$$

$$\Gamma^2_{21} = \Gamma^2_{12} = \frac{1}{2g}[g_{11}\frac{\partial g_{22}}{\partial \xi} - g_{12}\frac{\partial g_{11}}{\partial \eta}] \qquad (B-5)$$

$$\Gamma^2_{22} = \frac{1}{2g}[g_{11}\frac{\partial g_{22}}{\partial \eta} - g_{12}(2\frac{\partial g_{12}}{\partial \eta} - \frac{\partial g_{22}}{\partial \xi})] \qquad (B-6)$$

$$\Gamma^3_{\alpha\beta} = -\frac{1}{2}\frac{\partial g_{\alpha\beta}}{\partial \zeta}; \quad (\alpha,\beta = 1,2) \qquad (B-7)$$

$$\Gamma^1_{13} = \Gamma^1_{31} = \frac{1}{2g}[g_{22}\frac{\partial g_{11}}{\partial \zeta} - g_{12}\frac{\partial g_{12}}{\partial \zeta}] \qquad (B-8)$$

$$\Gamma^1_{23} = \Gamma^1_{3,2} = \frac{1}{2g}[g_{22}\frac{\partial g_{12}}{\partial \zeta} - g_{12}\frac{\partial g_{22}}{\partial \zeta}] \qquad (B-9)$$

$$\Gamma^2_{13} = \Gamma^2_{31} = \frac{1}{2g}[g_{11}\frac{\partial g_{12}}{\partial \zeta} - g_{12}\frac{\partial g_{11}}{\partial \zeta}] \qquad (B-10)$$

$$\Gamma^2_{23} = \Gamma^2_{32} = \frac{1}{2g}[g_{11}\frac{\partial g_{22}}{\partial \zeta} - g_{12}\frac{\partial g_{12}}{\partial \zeta}] \qquad (B-11)$$

$$\Gamma^3_{i3} = \Gamma^3_{3,i} = 0; \quad \Gamma^i_{33} = 0; \quad (i = 1,2,3) \qquad (B-12)$$

where $g = g_{11}g_{22} - (g_{12})^2$.

The covariant curvature tensor $b_{\alpha\beta}$ of the surface is related to the Christoffel symbols of the second kind by

$$b_{\alpha\beta} = \dot{\Gamma}^3_{\alpha\beta}; \quad (\alpha, \beta = 1, 2) \qquad (B-13)$$

where the dot superscript '$\cdot$' denotes a quantity on the body surface. From equation (B-7), the following expressions for $b_{\alpha\beta}$ result:

$$\begin{aligned} b_{11} &= -\frac{1}{2}\frac{\partial a_{11}}{\partial \zeta} \\ b_{22} &= -\frac{1}{2}\frac{\partial a_{22}}{\partial \zeta} \\ b_{12} = b_{21} &= -\frac{1}{2}\frac{\partial a_{12}}{\partial \zeta} \end{aligned} \qquad (B-14)$$

Appendix C

Principal Curvatures of the Surface

The principal curvatures K_1 and K_2 [equation (45)] play an important role in second-order boundary-layer theory since they indicate if the local radius of curvature of the surface is not negligible compared to the boundary-layer thickness. K_1 and K_2 are determined from the following relations [19]:

$$K_1 + K_2 = \frac{a_{11}b_{22} + a_{22}b_{11} - 2a_{12}b_{12}}{a_{11}a_{22} - (a_{12})^2} \qquad (C-1)$$

$$K_1 \cdot K_2 = \frac{b_{11}b_{22} - (b_{12})^2}{a_{11}a_{22} - (a_{12})^2} \qquad (C-2)$$

The Principal curvature radii R_1 and R_2 are given by

$$R_1 = \frac{1}{K_1} \qquad (C-3)$$

$$R_2 = \frac{1}{K_2} \qquad (C-4)$$

The directions of the principal curvatures of the surface λ_1 and λ_2 can be obtained as the solution of a quadratic equation [19]:

$$\lambda_{1,2} = \frac{b_{22}a_{11} - b_{11}a_{22}}{2(b_{11}a_{12} - b_{12}a_{11})} \pm \frac{\sqrt{(b_{11}a_{22} - b_{22}a_{11})^2 - 4(b_{11}a_{12} - b_{12}a_{11})(b_{12}a_{22} - b_{22}a_{12})}}{2(b_{11}a_{12} - b_{12}a_{11})} \qquad (C-5)$$

Acknowledgments

Financial support for this work was provided by NASA Lyndon B. Johnson Space Center under Contract No. NAS9-18493 with Dr. Chien-Peng Li as a technical monitor. The author wishes to express his sincere thanks to Dr. Frederick G. Blottner of Sandia National Laboratories and Dr. Carl D. Scott of NASA JSC for their valuable suggestions and comments.

References

[1] Li, C.-P., "Numerical Simulation of Entry Flow over Blunt Swept-Wing Planes," *Hypersonics,* Vol. II, edited by J.J. Bertin, J. Periaux and J. Ballmann, Birkhauser, Boston, 1992.

[2] Yee, H. C., "A Class of High-Resolution Explicit and Implicit Shock-Capturing Methods," NASA TM 101088, February 1989.

[3] DeJarnette, F. R. and Hamilton, H. H., "Inviscid Surface Streamlines and Heat Transfer on Shuttle-Type Configurations," J. Spacecraft, Vol. 10, No. 5, May 1973, pp. 314-321.

[4] Hamilton, H. H., DeJarnette, F. R. and Weilmuenster, K. J., "Application of Axisymmetric Analog for Calculating Heating in Three-Dimensional Flows," J. Spacecraft, Vol. 24, No. 4, July-August 1987, pp. 296-302.

[5] Harris, J. E., "An Implicit Finite-Difference Procedure for Solving the Three-Dimensional Compressible Laminar, Transitional, and Turbulent Boundary-Layer Equations," NASA SP-347, 1975, pp. 19-40.

[6] Cebeci, T., Kaups, K., Ramsey, J. and Moser, A., "Calculation of Three-Dimensional Compressible Boundary Layers on Arbitrary Wings," NASA SP-347, 1975, pp. 41-76.

[7] Kendall, R. M., Bonnett, W. S., Nardo, C. T. and Abbett, M. J., "Three-Dimensional Compressible Boundary Layers of Reacting Gases over Realistic Configurations," NASA SP-347, 1975, pp. 77-99.

[8] Blottner, F. G., "Computational Techniques for Boundary Layers," SAND-74-5821, 1974.

[9] Van Dyke, M., "Higher Approximations in Boundary-Layer Theory, Part I: General Analysis," J. Fluid Mech., Vol. 14, 1962, pp. 481-495.

[10] Van Dyke, M., "Higher Approximations in Boundary-Layer Theory, Part II: Parabola in Uniform Stream," J. Fluid Mech., Vol. 19, 1964, pp. 145-159.

[11] Van Dyke, M., "Second-Order Compressible Boundary Layer Theory with Application to Blunt Bodies in Hypersonic Flow," *Hypersonic Flow Research,* edited by F. R. Riddel, pp. 37-76, Academic Press, New York, 1962.

[12] Aupoix, B., Brazier, J. Ph. and Cousteix, J., "Asymptotic Defect Boundary-Layer Theory Applied to Hypersonic Flows," AIAA J., Vol. 30, No. 5, May 1992, pp. 1252-1259.

[13] Aupoix, B., Brajier, J. Ph., Cousteix, J. and Monnoyer, F., "Second-Order Effects in Hypersonic Boundary Layers," *The Third Joint Europe/US Short Course in Hypersonics,* RWTH Aachen, FRG,October 1990.

[14] Davis, R. T. and Flügge-Lotz, I., "Second-Order Boundary-Layer Effects in Hypersonic Flow Past Axisymmetric Blunt Bodies," J. Fluid Mech., Vol. 20, 1964, pp.593-623.

[15] Monnoyer, F., "The effect of Surface Curvature on Three-Dimensional, Laminar Boundary Layers," Doctoral Thesis, Universite libre de Bruxelles, 1985.

[16] Monnoyer, F., "Calculation of Three-Dimensional Attached Viscous Flow on General Configurations Using Second-Order Boundary-Layer Theory," Z. Flugwiss. Weltraumforsch. Vol. 14, 1990, pp. 95-108.

[17] Monnoyer, F., Mundt, Ch. and Pfitzner, M., "Calculation of the Hypersonic Viscous Flow past Reentry Vehicles with an Euler-Boundary Layer Coupling Method," AIAA Paper 90-0417, Reno, Nev., January 1990.

[18] Robert, K., "Higher-Order Boundary Layer Equations for Three-Dimensional, Compressible Flow," DLR-FB 77-36, 1977.

[19] Hirschel, E. H. and Kordulla, W., "Shear Flow in Surface-Oriented Coordinate," Vol. 4 in *Notes on Numerical Fluid Mechanics,* Vieweg Verlag, Braunschweig, 1981.

[20] Robert, K. and Grundmann, R., "Basic Equations for Non-Reacting Newtonian Fluids in Curvilinear, Non-Orthogonal, and Accelerated Coordinate Systems," DLR-FB 76-47, 1976.

[21] Sawley, M. L. and Wüthrich, "Non-Equilibrium Hypersonic Flow Simulation Using the Second-Order Boundary Layer Equations," Computer Methods in Applied Mechanics and Engineering, Vol. 89, 1991, pp. 129-140.

[22] Humphreys, D. A., "On the Identification of Active and Passive Terms in the Exact Viscous Flow Equations," The Aeronautical Research Institute of Sweden, FFA TN 1992-01, 1992.

[23] Panaras, A. G., "Boundary-Layer Equations in Generalized Curvilinear Coordinates," NASA TM-100003, August 1987.

[24] Steger, J. L., Van Dalsem, W. R., Panaras, A. G. and Rao, K. V., "A Formulation for the Boundary-Layer Equations in General Coordinates," NASA TM-100079, June 1988.

[25] Steger, J. L. and Van Dalsem, W. R., "Basic Numerical Methods," *Unsteady Transonic Aerodynamics:* Progress in Astronautics and Aeronautics, Vol. 120, edited by D. Nixon, AIAA, New York, 1989, pp. 133-209.

[26] Gershbein, E. A., "Asymptotic Solution of the Equations for a Three-Dimensional Multicomponent Laminar Boundary Layer with Large Injection," Izv. Akad. Nauk SSSR, Mekh. Zhidk. Gaza, No. 2, 1975.

[27] Shevelev, Yu. D., "Numerical Analysis of a Three-Dimensional Boundary Layer in a Compressible Gas," Izv. Akad. Nauk SSSR, Mekh. Zhidk. Gaza, No. 4, 1966.

[28] Howe, J. T., "Introductory Aerothermodynamics of Advanced Space Transportation Systems," AIAA Paper 83-0406, Reno, Nev., January 1983.

[29] Lee, J.-H., "Basic Governing Equations for the Flight Regimes of Aeroassisted Orbital Transfer Vehicles," *Thermal Design of Aeroassisted Orbital Transfer Vehicles:* Progress in Astronautics and Aeronautics, Vol. 96, edited by H. F. Nelson, AIAA, New York, 1985, pp. 3-53.

[30] Park, C., "A Review of Shock Waves around Aeroassisted Orbital Transfer Vehicles," NASA TM-86769, June 1985.

[31] Scott, C. D., "Effects of Thermochemistry, Nonequilibrium, and Surface Catalysis on the Design of Hypersonic Vehicles," *Hypersonics,* Vol. I: Defining the Hypersonic Environment, edited by J. J. Bertin, R. Glowinski and J. Periaux, Birkhauser, Boston, 1989, pp.355-427.

[32] Scott, C. D., "Wall Catalytic Recombination and Boundary Conditions in Nonequilibrium Hypersonic Flows - With Applications," *The Third Joint Europe/US Short Course in Hypersonics,* RWTH Aachen, FRG, October 1990.

[33] Deiwert, G. S., "Aerothermodynamics Research at NASA Ames Research Center," NASA TM-89439, September 1987.

[34] Anderson, D. A., Tannehill, J. C. and Pletcher, R. H., *Computational Fluid Mechanics and Heat Transfer,* Hemisphere Publishing Corp., Washington, D. C., 1984.

[35] Yang, H. Q., Habchi, S. D., and Przekwas, A. J., "A General Strong Conservation Formulation of Navier-Stokes Equations in Non-Orthogonal Curvilinear Coordinates," AIAA Paper 92-0187, Reno, Nevada, January 1992.

[36] Park, C., "Assessment of a Two-Temperature Kinetic Model for Dissociating and Weakly Ionizing Nitrogen," J. Thermophysics, Vol. 2, No. 1, January 1988, pp. 8-16.

[37] Park, C., "Assessment of Two-Temperature Kinetic Model for Ionizing Air," J. Thermophysics, Vol. 3, No. 3, July 1989, pp. 233-244.

[38] Lee, J.-H., "Electron-Impact Vibrational Excitation Rates in the Flowfield of Aeroassisted Orbital Transfer Vehicles," *Thermophysical Aspects of Re-entry Flows:* Progress in Astronautics and Aeronautics, Vol. 103, edited by J. N. Moss and C. D. Scott, AIAA New York, 1986, pp. 197-224.

[39] Lee, J.-H., "Electron-Impact Vibrational Relaxation in High-Temperature Nitrogen," AIAA Paper 92-0807, Reno, Nevada, January 1992. Also to be published in J. Thermophysics.

[40] Gnoffo, P. A., Gupta, R. N. and Shinn, J. L., "Conservation Equations and Physical Models for Hypersonic Air Flows in Thermal and Chemical Nonequilibrium," NASA TP-2867, February 1989.

[41] Thareja, R., Szema, K. Y. and Lewis, C. H., "Viscous Shock-Layer Predictions for Hypersonic Laminar or Turbulent Flows in Chemical Equilibrium over the Windward Surface of a Shuttle-Like Vehicle," AIAA Paper 82-0201, Orlando, FL., January 1982.

[42] Kim, M. D., Swaminathan, S. and Lewis, C. H., "Three-Dimensional Nonequilibrium Viscous Shock-Layer Flow over the Space Shuttle Orbiter," J. Spacecraft, Vol. 21, No. 1, 1984.

[43] Thompson, R. A., "Three-Dimensional Viscous Shock Layer Applications for the Space Shuttle Orbiter," *Thermophysics in Astronautics and Aeronautics:* Progress in Astronautics and Aeronautics, Vol. 103, edited by J. N. Moss and C. D. Scott, AIAA, New York, 1986, pp. 541-570.

[44] Thompson, R. A., "Comparison of Nonequilibrium Viscous-Shock-Layer Solutions with Windward Surface Shuttle Heating Data," AIAA Paper 87-1473, Honolulu, Hawaii, June 1987.

[45] Davis, R. T., "Numerical Solution of the Hypersonic Viscous Shock-Layer Equations," AIAA J., Vol. 8 No. 5, May 970, pp. 843-851.

[46] Okuno, A. F. and Park, C., "Stagnation-Point Heat-Transfer Rate in Nitrogen Plasma Flows: Theory and Experiment," Trans. ASME, Ser. C: J. Heat Transfer., Vol. 92, No. 3, Aug. 1970, pp 372-384.

[47] Lighthill, M. J., "On Displacement Thickness," J. Fluid Mech. Vol. 4, pp. 383-392, 1958.

[48] Balakrishnan, A., "Correlations for Specific Heats of Air Species to 50,000 K," AIAA Paper 86-1277, Boston, Mts., June 1986.

[49] Yos, J. M., "Transport Properties of Nitrogen, Hydrogen, Oxygen, and Air to 30,000 K," Technical Memorandum RAD TM-63-7, AVCO-RAD, Wilmington, Mass., Mar. 1963.

[50] Gupta, R. N., Yos, J. M., Thompson, R. A. and Lee, K.-P., "A Review of Reaction Rates and Thermodynamic and Transport Properties for an 11-Species Air Model for Chemical and Thermal Nonequilibrium Calculations to 30000 K," NASA RP-1232, Aug. 1990.

[51] Park, C., "A Review of Reaction Rates in High Temperature Air," AIAA Paper 89-1740, Buffalo, NY., June 1989.

[52] Park, C., "Convergence of Computation of Chemical Reacting Flows," *Thermophysical Aspects of Re-entry Flows:* Progress in Astronautics and Aeronautics, Vol. 103, edited by J. N. Moss and C. D. Scott, AIAA, New York, 1986, pp. 478-513.

[53] Park, C., "Problems of Rate Chemistry in the Flight Regimes of Aeroassisted Orbital Transfer Vehicles," *Thermal Design of Aeroassisted Orbital Transfer Vehicles:* Progress in Astronautics and Aeronautics, Vol. 96, edited by H. F. Nelson, AIAA, New York, 1985, pp. 511-537.

[54] Millikan, R. C. and White, D. R., "Systematics of Vibrational Relaxation," J. of Chem. Phys., Vol. 39, No. 12, Dec. 1963, pp. 3209-3213.

[55] Candler G. and Park, C., "The Computation of Radiation from Nonequilibrium Hypersonic Flows," AIAA Paper 88-2678, San Antonio, TX., June 1988.

[56] Li, C.-P., Private Communication, 1992.

[57] Rakich, J. V. and Mateer, G. G., "Calculation of Metric Coefficients for Streamline Coordinates," AIAA J., Vo. 10, No. 11, November 1972, pp. 1538-1540.

[58] DeJarnette, F. R. and Hamilton, H. H., "Aerodynamic Heating on 3-D Bodies Including the Effects of Entropy-Layer Swallowing," J. Spacecraft, Vol. 12, No. 1, January 1975, pp. 5-12.

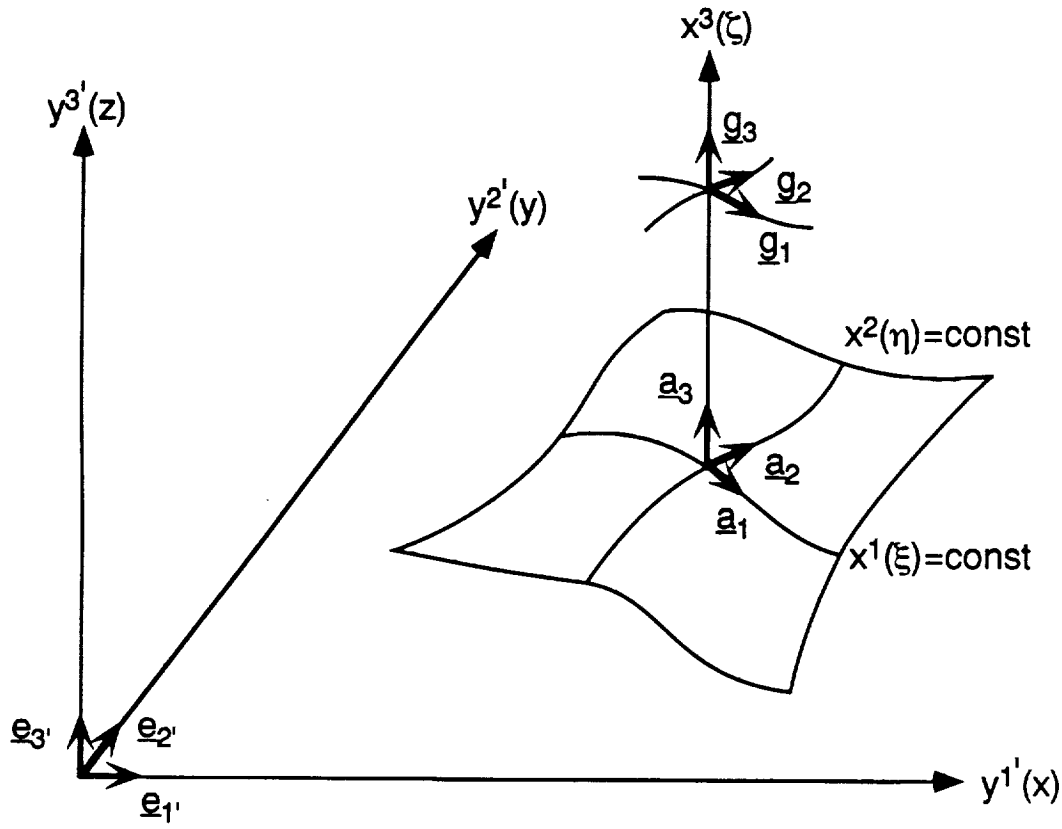

Fig. 1 Orientation of coordinate systems.
($y^{i'}(x,y,z)$: Cartesian coordinate system;
$x^{i}(\xi,\eta,\zeta)$: Curvilinear surface-oriented coordinate system)

REPORT DOCUMENTATION PAGE

Form Approved
OMB No. 0704-0188

1. AGENCY USE ONLY *(Leave blank)*	2. REPORT DATE	3. REPORT TYPE AND DATES COVERED
	February 1993	NASA Contractor Report

4. TITLE AND SUBTITLE
Hypersonic Three-Dimensional Nonequilibrium Boundary-Layer Equations in Generalized Curvilinear Coordinates

5. FUNDING NUMBERS
NAS9-18493

6. AUTHOR(S)
Jong-Hun Lee

7. PERFORMING ORGANIZATION NAME(S) AND ADDRESS(ES)
BSA Services
Houston, TX 77045

8. PERFORMING ORGANIZATION REPORT NUMBER

9. SPONSORING / MONITORING AGENCY NAME(S) AND ADDRESS(ES)
National Aeronautics and Space Administration
Washington, DC 20546-0001

10. SPONSORING / MONITORING AGENCY REPORT NUMBER
CR-185677

11. SUPPLEMENTARY NOTES

12a. DISTRIBUTION / AVAILABILITY STATEMENT
Unclassified - Unlimited

12b. DISTRIBUTION CODE

13. ABSTRACT *(Maximum 200 words)*

The basic governing equations for the second-order three-dimensional hypersonic thermal and chemical nonequilibrium boundary layer are derived by means of an order-of-magnitude analysis. A two-temperature concept is implemented into the system of boundary-layer equations by simplifying the rather complicated general three-temperature thermal gas model. The equations are written in a surface-oriented non-orthogonal curvilinear coordinate system, where two curvilinear coordinates are non-orthogonal and a third coordinate is normal to the surface. The equations are described with minimum use of tensor expressions arising from the coordinate transformation, to avoid unnecessary confusion for readers. The set of equations obtained will be suitable for the development of a three-dimensional nonequilibrium boundary-layer code. Such a code could be used to determine economically the aerodynamic/aerothermodynamic loads to the surfaces of hypersonic vehicles with general configurations. In addition, the basic equations for three-dimensional stagnation flow, of which solution is required as an initial value for space-marching integration of the boundary-layer equations, are given along with the boundary conditions, the boundary-layer parameters and the inner-outer layer matching procedure. Expressions for the chemical reaction rates and the thermodynamic and transport properties in the thermal nonequilibrium environment are explicitly given.

14. SUBJECT TERMS	15. NUMBER OF PAGES
Hypersonic flow; three-dimensional boundary layer; non-orthogonal curvilinear coordinates; thermochemical nonequilibrium; two-temperature model	62
	16. PRICE CODE

17. SECURITY CLASSIFICATION OF REPORT	18. SECURITY CLASSIFICATION OF THIS PAGE	19. SECURITY CLASSIFICATION OF ABSTRACT	20. LIMITATION OF ABSTRACT
Unclassified	Unclassified	Unclassified	Unlimited